DOE Award Number: DE-NE0000542

Recipient: Lockheed Martin Corporation

Project Title: Nuclear Energy Enabling Technologies
Advanced Methods for Manufacturing

Date of Report: 31 December 2015

Report/Deliverable: Final Technical Report on Laser Direct Manufacturing (LDM) for Nuclear Power Components

Technical POC:	Contractual Administration POC:
Scott A. Anderson Advanced Technology Center 9100 Ashton Ave., Manassas, VA 20110 Scott.Anderson@lmco.com 571.292.3005 (office) 571.358.1954 (mobile)	Carlos Uriarte Advanced Technology Center 3251 Hanover Street, Palo Alto, CA 94304 carlos.g.uriarte@lmco.com 650.424.2676 (office) 650.424.3066 (office)

1.0 Executive Summary

Lockheed Martin (LM) has been a leader since the 1990s in the development and implementation of Laser Direct Manufacturing (LDM) processes, including the adaptation to articles on the well-known F-35 Fifth Generation Jet Fighter and the next generation human spacecraft, the Orion Multi-Purpose Crew Vehicle. The objective of this project is to extend LDM expertise, developed for the aero-space industry, towards manufacturing nuclear power reactor components that demonstrate accelerated schedule for deployment with the cost and fabrication benefits of improved radiation resistance over standard state of the art components.

The Direct Metal Laser Sintering (DMLS) used for fabricating parts on this project is a powder bed method using a stationary bed of metal powder as the base layer for the build. A series of experiments varying build process parameters (scan speed and laser power) was conducted at the outset to establish the optimal build conditions for each of the alloys. Fabrication was completed in collaboration with Quad City Manufacturing Laboratory (QCML). The density of all sample specimens was measured and compared to literature values. Optimal build process conditions giving fabricated part densities close to literature values were chosen for making mechanical test coupons. Test coupons whose principal axis is on the x-y plane (perpendicular to build direction) and on the z plane (parallel to build direction) were built and tested as part of the experimental build matrix to understand the impact of the anisotropic nature of the DMLS process.

For most materials, the microstructure is dependent on alloy composition and thermal history. The microstructure in turn determines the mechanical properties. Additive manufacturing offers more flexibility in optimizing process conditions and alloy microstructure leading to better control of mechanical properties. Test and characterization studies were performed that evaluated the anisotropic behavior of the materials based on build orientation and post processing methodologies. Strong anisotropic behavior of the material and mechanical properties based on grain orientations were observed. Demonstration articles based on a notional nuclear fuel spacer grids were fabricated in 316L SS and three Inconel alloys (600, 718, 800) to demonstrate complex design fabrications in multiple relevant alloys. Better understanding of the manufacturing process, article qualification challenges and the business case value addition from LDM enables faster adoption of additive approaches for the nuclear industry.

For the nuclear industry, laser direct manufacturing promises faster build schedules and reduced costs. Novel and challenging parts for improved performance can be tested quickly and with high fidelity. Digital design optimization can be combined with simulation to dramatically improve new reactor designs, fluid flow performance and overall reactor safety. Additive manufacturing is changing the way all industries view manufacturing and the nuclear industry is well positioned to reap the benefits.

2.0 Program Overview / Accomplishments

Current light-water nuclear reactors cost >$10B/unit with a significant portion of that cost associated with manufacturing and assembly. Next-generation concepts for Small Modular Reactors (SMR) are estimated to reduce that cost to <$2B/unit and enable rapid fielding. A $700B international market exists for nuclear power plant equipment and services over the next ten years and the Department of Energy (DOE) has identified advanced manufacturing methods

as a key enabler to achieve affordability. The DOE has thus established the Nuclear Energy Enabling Technologies – Advanced Manufacturing Methods (NEET-AMM) initiative.

Lockheed Martin was awarded contract DE-NE0000542 under the NEET-AMM initiative in late 2012 to demonstrate the cost and schedule benefits of additive manufacturing for fabrication of nuclear reactor components and assemblies and leverage our expertise in this domain to transition the technology to the nuclear sector.

The original goals of the program were (i) to demonstrate laser direct manufacturing techniques for baseline and advanced radiation tolerant alloys, (ii) to develop novel alloys that leverage the rapid quench rates offered by laser direct manufacturing and further enhance radiation tolerance, and (iii) to demonstrate nuclear power component level hardware using laser direct manufacturing techniques.

By applying demonstrated experience for building manufacturing case studies of LDM-fabricated components with sophisticated requirements, this study begins to define the implementation path for nuclear energy advanced manufactured components. Additionally, the LDM advantages that inherently allow microstructure control to improve nuclear power generation plant performance were validated with industry specific formulations. Figure 1 highlights the program schedule and highlighted objectives to meet the program goals.

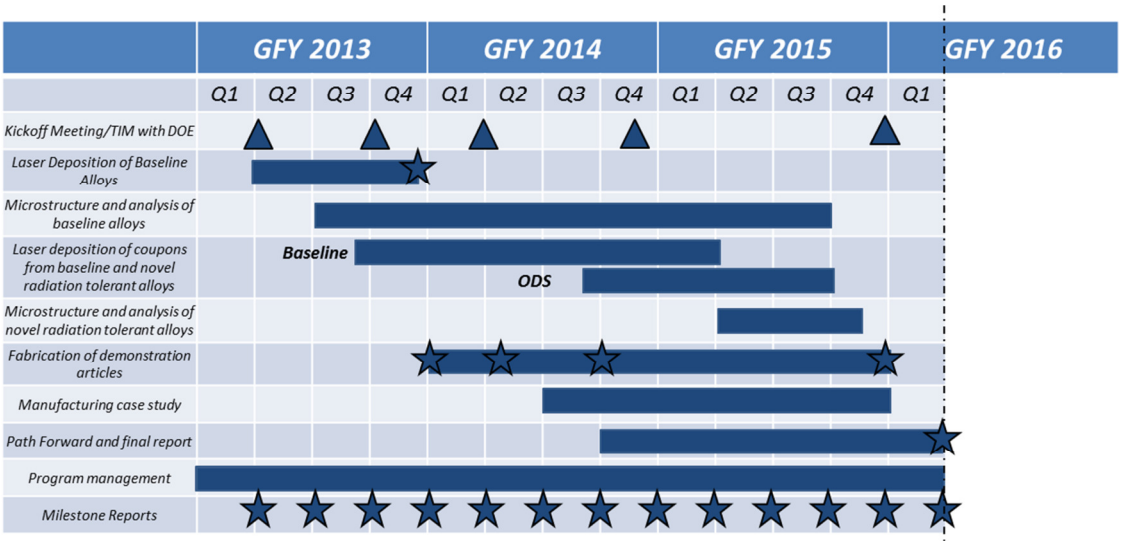

Figure 1. Program Schedule with Objectives, Milestones and Reporting

For each of the identified program objectives in Figure 1, challenges and associated mitigations were encountered and implemented as the effort matured during the three year period of performance. Table 1 highlights the major challenges, mitigations and program accomplishments.

Table 1. Program Objectives and Accomplishments

Original Objective	Challenges / Mitigations	Accomplishments
Develop an LDM Baseline Alloy Approach, Fabricate Samples, and Perform Material Characterization	• Difficulty engaging NE primes and supply chain for tech transition	• Completed tooling assessment for LDM approach • Completed process development and processing using LDM for 316L SS at QCML • Completed characterization case study 316L SS

Development of LDM Approach for Radiation Tolerant Alloys	• Raw materials (e.g., Inconel 800) had long lead times • ODS alloy powder formulation was a challenge	• Completed material trade study and process optimization for Inconel alloys • Completed process development and sample fabrication for Inconel 600, 718, 800 • Completed characterization Inconel 600 case study • XRD verification of differential crystallinity • Produced ODS alloy powder for LDM processing • Completed initial ODS alloy process development, fabrication & characterization
Fabricate Demonstration Articles	• Difficulty getting proprietary designs of reactor internal components for demo • Internally developed notional design and CAD drawings	• Developed LDM approach for complex fuel rod spacer grid • Completed thin wall study for SS and Inconel alloys • Fabricated 3x3, 10x10, 15x15 spacer grids
Manufacturing Case Study that Demonstrates Schedule and Cost Benefits of LDM	• Initial assessments highlighted LDM value prop. as highly part specific • Considerations taken in case study to address part-by-part specificity	• Evaluated cost drivers and assessed between additive and traditional manufacturing methods • Assessed value drivers for LDM • Identified path forward items to build strategic roadmap for nuclear technology development
Program Management	• Slow program startup - year 1 • Recovered with activity surge • Personnel overturn with loss of original PM and tech lead. • Back-filled with new personnel	• Completed program reporting milestones and deliverables • Presentation given at Nov. 2014 ANSI NESCC • Presentation given at June 2015 Tech Connect • Initiated collaboration for irradiation and PIE of LDM samples with Texas A&M

As part of the fabrication and sample testing approach, 316L stainless steel (SS), Inconel alloys 600, 718 and 800 and oxide dispersion strengthened (ODS) steel articles were fabricated. Materials based case studies and demonstration articles were completed for the 316L SS and the Inconel 600. For the Inconel 718 and 800 alloys, material samples and demo articles were fabricated, and material samples were fabricate for the ODS steel. Table 2 shows the completion matrix for the five alloys.

Table 2. Sample and Demo Development Matrix for Alloys Used in Program.

	Inconel 600	Inconel 718	Inconel 800	316L SS	ODS 316L SS
LDM Trials	Complete	Complete	Complete	Complete	Complete
Microstructures	Complete	N/C	N/C	Complete	Complete
Mechanical Properties	Complete	N/C	N/C	Complete	N/C
Test Specimens	Complete	Complete	Complete	Complete	Complete
Demo Articles	Complete (3x3*, 10x10 and 15x15)	Complete (3x3*)	Complete (3x3*)	Complete (3x3)	N/A

** Baseline 3x3 and thin wall demo samples*

3.0 Program Activities

The international roadmap for the next generation of fission nuclear reactors under development (Generation IV) has six advanced reactor concepts under consideration. In comparison to earlier generations of nuclear reactor systems, all Generation IV reactor concepts have in their designs a higher operating temperature and a higher radiation flux. Figure 2 lists the six advanced reactor concepts along with their temperature and dose regimes of operation [1]. Apart from thermodynamic efficiency, reduced construction and operating costs are factors under consideration in the development of Generation IV power plants.

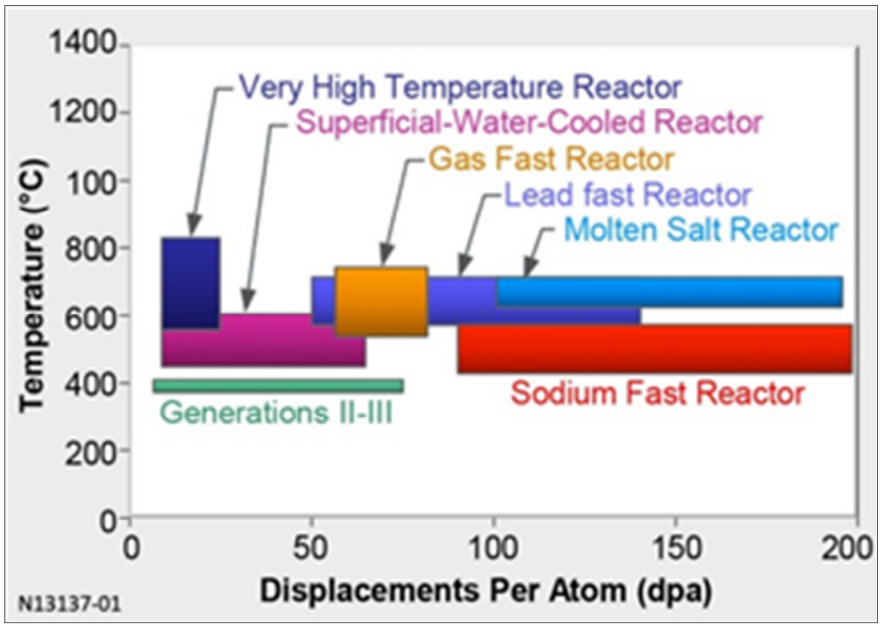

Figure 2. Temperature and dose regimes for the operation of the six advanced reactor concepts for next generation nuclear power reactors [1].

Fabrication of components for the reactor core, where fission reactions and thermal energy transfer to coolant occurs, poses significant materials challenges for the advanced reactor concepts. The neutron spectrum contributing to displacement damage quantified by displacements per atom (dpa) from these concepts include both "fast" neutrons with energies near 1-2 MeV as well as "thermal" neutrons with energies near ~1 eV. A general fuel assembly configuration used in light water reactor, supercritical water reactor, sodium fast reactor, lead fast reactor and variants of the gas fast reactor designs is shown in Figure 3. [1] Apart from the cladding and duct materials which have to withstand the extreme operating conditions indicated in Figure 2, seemingly simple components such as plumbing, fittings, valve housings, ducting, brackets and vessels must also survive aggressive radiation environments, high temperatures, thermal cycles and pressurized flow for 40 or more years. Many different classes of materials have been studied in an effort to meet these performance challenges. Among them, advanced specialized stainless steels have been critical to servicing the needs for many of the core as well as out-of-core components.

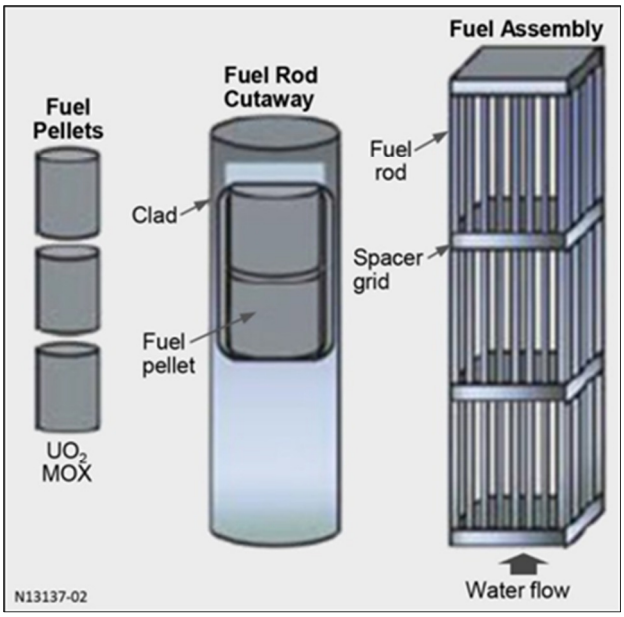

Figure 3. General fuel assembly configuration for fuel and coolant; the requirements for core components used in this general configuration is used as guidance for selection of the advanced nano-phase materials that are discussed in this report.

Most of these nuclear alloy materials utilize process-structure-property relationships to optimize microstructure for improved performance. Another approach is to use processing techniques such as direct manufacturing for advanced alloy development and component fabrication.

3.1 Additive Manufacturing Methods for Reactor Assemblies and Components

As with the development of advanced materials, manufacturing techniques have also advanced. Advanced manufacturing (AM) techniques are being used to build production parts. The unique benefits of near net shape manufacturing, increased geometrical freedom, and ability to control microstructure have led to dramatic reductions in part cost and lead time. The various types of AM technologies include powder-based processes, liquid-based processes and solid-based process each with its own benefits and targeted materials. AM powder based processes are used with metals, polymers and ceramics.

Metal powder based LDM is the technique of choice for alloy development and component fabrication. Figure 4 shows a fuel rod spacer grid demonstration article being built with LDM using 316L stainless steel. LDM is a laser-hybrid welding process which builds structure in an additive manner by layering metal alloy in specific near-net shapes with robotic control. After deposition, the near-net shape component is machined to final tolerance. To address the manufacturing and operating cost as well as lead time issues of component manufacturing, traditional machine shop operations such as machine from billet, machine from forging or casting need to be replaced with Advanced Manufacturing Methods (AMM).

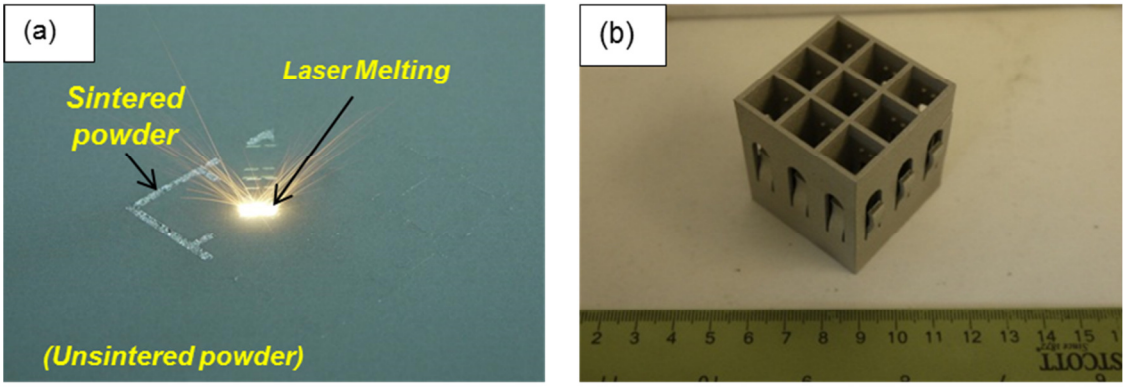

Figure 4. (a) Fuel rod spacer grid demonstration article in build; (b) demonstration article.

Lockheed Martin Space Systems Company (LMSSC)- Advanced Technology Center (ATC) has partnered with Quad City Manufacturing Laboratories (QCML) to achieve the goals of this project. QCML is headquartered in Rock Island Arsenal in Rock Island, Illinois. QCML is a research and development laboratory that is used to taking the R&D to the technology transfer state. They are well versed in advanced materials and additive manufacturing processes such as Direct Laser Sintering (DMLS), Laser Additive Manufacturing (LAM) Spark Plasma Sintering (SPS), Friction Stir Welding (FSW), and Hot Isostatic Pressing (HIP). QCML utilized their knowledge and equipment to support the LDM fabrication of samples and demonstration components. Two specific systems were used the DMLS powder bed method and the Laser Engineered Net Shaping (LENS) nozzle powder delivered system (LENSTM-850 System). Schematics of both systems can be seen in Figure 5.

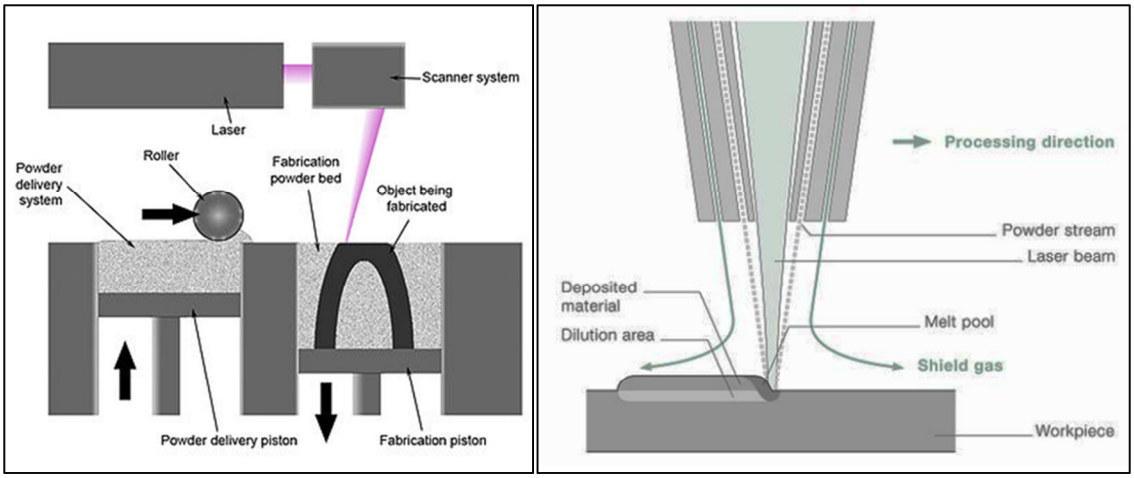

Figure 5. Schematic showing the powder bed method (left) and nozzle powder delivered method (right) LDM systems available for use.

In the powder bed Laser Direct Manufacturing method, a stationary bed of powdered metal is used as the base for the layered build. The heat source such as a laser spot rapidly 'draws' the image of the layer section in the powder bed, fusing the material into a solid structure. The bed is indexed a small distance, and a doctor blade scrapes a new layer of powder over the surface. The build continues with another melting and fusing powder into shaped structure. Structures built with powder bed method are typically Hot Isostatic Pressed (HIP) to reduce probability of void presence. The beam deposition that is used for rapid large scale builds has excellent

microstructure control but has poor feature resolution and has difficulty producing complex shapes. With the LENS nozzle powder delivered method; the multi-axis position head delivers the metal powder and houses the laser. This allows for application of the powder directly to the region of the beam and melt-pool. The resultant comparison of the two systems indicates that the direct metal laser sintering (DMLS) is the fastest most flexible approach while the LENS system is very well suited for repairing existing parts that require higher positional accuracy with the most flexibility. Comparison of the two techniques is in shown in Table 3.

Table 3. Comparison of Metal AM Technologies (Powder Bed Fusion vs. Beam Deposition)

Characteristic	Powder Bed Fusion (PBF)	Beam Deposition (BD)
Energy Source	High-power laser or electron beam	High-power laser or electron beam
Atmosphere	Vacuum or inert gas	Vacuum or shielding gas
Materials	Metals, polymers, ceramics	Metals
Material Form	Powder	Powder or wire
Material Feed	Movable powder bed	Multi-axis deposition head
Powder Fusion	Full melting, liquid-phase, solid-state, or chemically-induced	Full melting
Build Rate	Moderate	Moderate to slow
Feature Resolution	Excellent to moderate	Moderate to poor
Surface Finish	Excellent to poor	Moderate to poor
Strengths	Can build multiple parts simultaneously, good feature resolution, can easily fabricate complicate geometries	Can fabricate large structures, excellent control of microstructure, can be used to add features to or repair existing parts
Limitations	Part size limited by size of chamber, difficult to control microstructure, residual stress buildup, some post processing required	Difficulty processing complex geometries, poor feature resolution and surface finish, requires significant post-processing
Best Suited For	Low to medium volume production of small, geometrically-complex parts	Fabrication of large structures that are difficult or costly to make via conventional methods; adding high-value features to simple components

The powder bed method was selected to build the metallurgical and the mechanical test specimens for the majority of this effort. The DMLS powder bed technique has excellent feature resolution and makes complex geometries with ease. This method is the method of choice for alloy development.

An EOS M270 Extended-Titanium system was used to fabricate Alloy 600, Alloy 718, Alloy 800, and 316L stainless steel specimens in this study. This system is classified as a powder bed fusion (PBF) additive manufacturing process and is shown in Figure 6.

Figure 6. EOS M270 powder bed fusion system used to fabricate specimens in this study.

Some experimental work was also performed on a direct energy deposition (DED) system, which is sometimes referred to as a Laser Engineered Net-Shaping (LENS) tool. The powder bed fusion process requires more powder, is slower, but can produce parts with a significantly higher resolution than the direct energy deposition process. The PBF process utilizes substantially thinner layers than the DED process. Both processes utilize spherical powders, but the PBF process uses a smaller particle size (typically under 45 microns) than the DED process (typically 45-100+ microns). Figure 7 is a photograph of the DED process during fabrication.

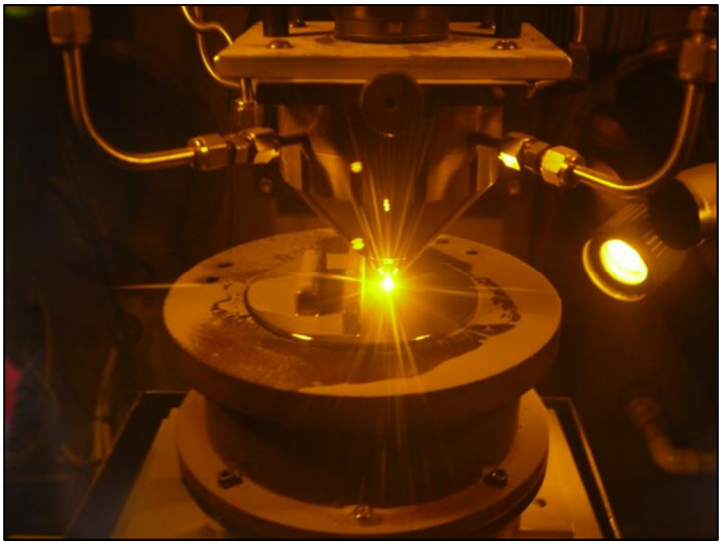

Figure 7. Direct Energy Deposition System (DED)—sometimes referred to as a Laser Engineered Net-Shaping (LENS) system.

While determining the best technique to use for build was import, equally important was to review and determine the materials for fabricating the test specimens to be used with the additive manufacturing process.

3.2 Materials Development and Characterization

3.2.1 Selection to Improve Radiation Tolerance of Traditional Reactor Alloys

A trade study was conducted to look at the various classes of nuclear reactor alloy materials being studied for next generation nuclear systems. Allen et. al. give a detailed description of material needs for cladding, duct and structural components of nuclear reactors [2]. These materials needs are derived from the higher temperature and dose regimes of operation for future reactor concepts as shown in Figure 2. The requirements, listed in Table 4, provide a basis for comparison between alloys being considered as alternatives. These challenging requirements represent the outer limit; out-of-core component materials are not expected to satisfy all of these requirements.

Table 4. Comparison Criteria in Selection of Alternate Nuclear Reactor Alloy Materials

1	Low neutron absorption
2	Elevated temperature mechanical properties • Creep resistance • Long-term stability • Compatibility with reactor coolant
3	Resistance to irradiation-induced damage (greater than 200 dpa) • Radiation hardening and embrittlement • Void swelling • Creep • Helium-induced embrittlement (HTGR) • Phase instabilities

Allen et. al. also give a comprehensive review of the materials development conducted as part of the United States National Cladding and Duct Development program (USNCDDP) as well as summary highlights from the international fast reactor programs, the fossil power generation industry, and the fusion energy materials program that have led to improvements in alloying of advanced steels. The USNCDDP studies focused on irradiation effects in three classes of materials: austenitic alloys, ferritic alloys and precipitation hardened Fe-Ni alloys. The strengths and weaknesses of each class of materials based on this study was documented providing a significant database for further material developments.

The ferritic steel HT9 was selected as the best candidate based on this study for the sodium cooled fast reactor facility (FFTF). HT9 along with another commercial ferritic-martensitic steel T91 were studied as suitable alloys for core components as part of the Advanced Fuel Cycle Initiative program. The Fossil Fuel Materials Development programs have developed ferritic-martensitic steels with higher temperature capability such as NF616 and HCM12A. Reduced-activation steels with 7-9% chromium and having vanadium, tungsten and tantalum were developed in the Fusion Materials Development programs.

Through its use in many of the developmental programs in the last few decades, a comprehensive database on material performance and understanding of material behavior for HT9 and T91, both of which have good resistance to void swelling, is available in literature. Among the Nickel alloys, which have higher strength and better corrosion resistance, Inconel 800H is a candidate material for Generation IV systems [3]. Following the accident at Fukushima Daiichi in 2011, resulting from hydrogen buildup caused by reaction of Zirconium alloy cladding with high-temperature, high-pressure steam, there is continued interest in steels as alternate nuclear alloys [4].

Introduction of stable nanoscale phases of carbides, nitrides and oxides is another method of obtaining high-temperature strength. In Oxide-Dispersion Strengthened (ODS) steels, Y_2O_3 particles are mechanically milled with ferritic alloy giving a fine dispersion of Y_2O_3 nanoclusters that are stable to high operating temperatures [5]. New formulations for ODS steels continue to be studied to improve performance before and after irradiation [6]. High-Temperature Ultrafine-Precipitation-Strengthened (HT-UPS) steels are another example of nanoscale carbide precipitates giving high temperature strength and creep resistance. Unlike ODS steels, HT-UPS steels are produced with standard alloy production techniques that use thermomechanical processing conditions along with alloy composition control to create the nanoscale carbide precipitates. The nanometer domains mitigate irradiation damage through pinning dislocations and also creating traps for radiation-produced defects. Modeling efforts have simulated the phenomenological response of these domains in presence of induced radiation defects providing understanding of time scales, length scales of interactions and providing targets for grain size and grain boundary microstructure features [7].

Based on the literature review four classes of materials were identified for a first round of development with our Direct Manufacturing techniques.

1) HT9 or later generations of F/M steels as a good baseline alloy to build control samples
2) ODS steels to examine effect of direct manufacturing methods on nanoscale oxide domains.
3) Inconel 800 series of materials to study the effect of processing parameters offered by direct manufacturing methods to improve performance under irradiation. .
4) Among the refractory alloys, the Mo (TZM) alloys have a high operating temperature window and also, the most information on irradiated material properties.

The material selection was further reduced after assessment of the Trade Study and two technical reviews. The experimental matrix for trial runs focused on two classes of alloys: stainless steels for a baseline case and the Inconel/Incoloy series and the ODS material.

Among the steels, the 300-series stainless steels have been chosen because of the general use of Type 316 and Type 304 in many reactor components as compared to HT-9, a 12Cr-1Mo-VW steel which was originally proposed in the trade study and which is principally used for the reactor core components.

The availability of the *316L* powder in the particle size specification needed for compatibility with QCML Electro Optical Systems (EOS) system for DMLS was another factor in its choice for experimental trials. The Inconel/Incoloy series, *Alloy 600, Alloy 718, and Alloy 800* were the three alloys that were selected and procured for the direct manufacturing build trials. ODS steels were not readily available for purchase, as an alternative, Yttria (Y_2O_3) powder was purchased separately to be milled with 316L steel, to examine the nanoscale oxide domains. Most of these alloys are addressed for nuclear construction in the ASME Boiler and Pressure Vessel Code.

The six powders used were characterized with Scanning Electron Microscopy (SEM) and Energy Dispersive Spectroscopy EDS. The SEM and EDS information can be found in Table 5. The data have not been verified by a standard.

Table 5. SEM Images and EDS Composition of Each of the Powders Used to Build Samples

Powder	EDS - Composition
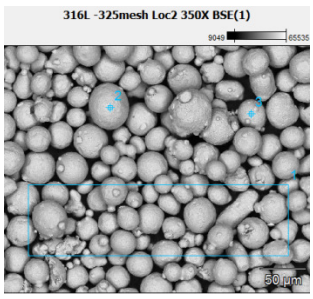 316L Stainless Steel -325 mesh	
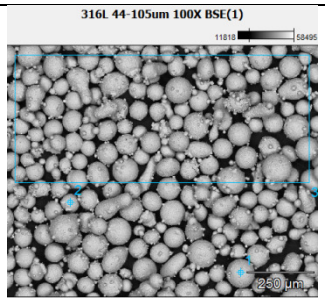 316L Stainless Steel 44-105Um	
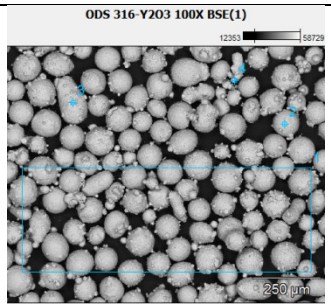 ODS Steel (316L SS 44-105um) Ball milled powder	
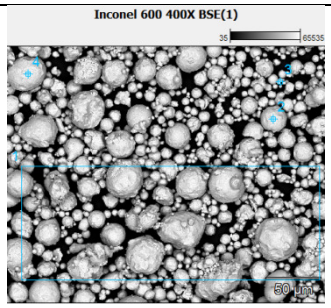 Inconel 600	

	Si	S	Cr	Mn	Fe	Ni	Mo
316L -325mesh pt1	0.6	0.0	18.0	2.2	Bal	9.5	1.5
316L -325mesh pt2	0.5	0.1	17.3	1.7	Bal	9.7	1.8
316L -325mesh pt3	0.6	0.2	17.0	1.7	Bal	9.1	1.6
316L Spec	1	0.03	16-18	2	Bal	10-14	2-3

	Si	S	Cr	Mn	Fe	Ni	Mo
316L 44-105um pt1	0.7	0.1	16.9	1.5	Bal	9.6	1.7
316L 44-105um pt2	0.6	0.0	18.5	1.6	Bal	14.3	2.0
316L 44-105um pt3	0.5	0.5	18.2	2.3	Bal	10.8	1.0
316L Spec	1	0.03	16-18	2	Bal	10-14	2-3

	O	Si	S	Cr	Mn	Fe	Ni	Y	Mo
ODS 316-Y2O3 pt1	5.0	0.6	0.3	16.0	1.8	59.2	8.9	7.3	0.9
ODS 316-Y2O3 pt2	4.5	0.6	0.2	15.3	1.6	60.4	9.8	6.5	1.2
ODS 316-Y2O3 pt3	4.3	0.7	0.0	15.1	1.2	64.8	10.1	2.3	1.6
ODS 316-Y2O3 pt4	1.4	0.2	0.0	16.5	2.4	66.4	7.5	5.2	0.4
No Spec for ODS									

	Si	S	Cr	Mn	Fe	Ni	Cu
Inconel 600 pt1	0.5	0.0	15.0	1.3	7.6	75.6	0.0
Inconel 600 pt2	0.3	0.0	15.2	0.7	8.4	75.3	0.0
Inconel 600 pt3	0.2	0.0	15.3	0.8	7.4	76.3	0.0
Inconel 600 pt4	0.5	0.0	15.9	1.1	8.1	74.3	0.1
Inconel 600 Spec	0.5	0.015	14-17	1.0	6-10	72-76	0.5

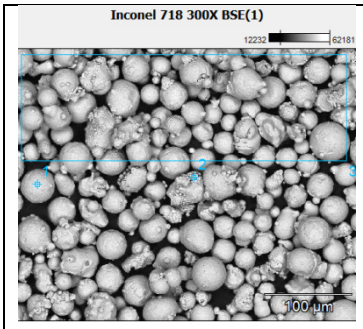

Inconel 700

	Al	Ti	Cr	Mn	Fe	Ni	Cu	Nb	Mo
Inconel 718 pt1	0.7	0.9	20.2	0.0	19.4	52.8	0.1	2.7	3.0
Inconel 718 pt3	0.4	0.8	20.2	0.1	20.1	53.0	0.0	3.0	1.9
Inconel 718 Spec	0.5	0.9	19	--	18.5	52.5	0.15	5.1	3

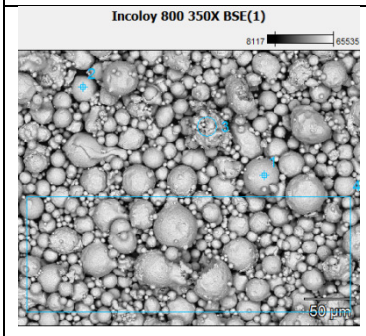

Incoloy 800

	Al	Si	Ti	Cr	Mn	Fe	Ni	Cu
Incoloy 800 pt1	0.3	0.5	0.5	21.1	1.2	44.7	31.7	0.0
Incoloy 800 pt2	0.5	0.8	0.5	21.7	1.4	42.4	32.6	0.1
Incoloy 800 pt3	0.3	0.5	0.7	21.8	1.2	44.0	31.7	0.0
Incoloy 800 pt4	0.3	0.5	0.5	23.5	2.0	43.3	29.6	0.2
Incoloy 800 Spec	.15-.6	0.5	.15-.6	19-23	0.75	39.5min	30-35	0.38

3.2.2 Fabrication of Test Articles Using Radiation Tolerant Alloys

In an effort to successfully meet the objectives of this effort by utilizing LDM techniques to build nuclear power component hardware level and to develop novel alloys that leverage the rapid quench rates offered by laser direct manufacturing and further enhance radiation tolerance test articles for microstructure examination and mechanical properties had to be fabricated.

Fabrication of the test samples had to take into consideration the type of process selected (powder bed fusion), the types of materials selected (316L SS and the Inconel/Incoloy alloys), as well as the process parameter variables scan speed and laser power. A series of experiments was conducted to assess the impact of the anisotropic nature of the DMLS process. Upon characterization of the samples the effects of the laser power and scan speed on the coupons whose principal axis is on the x-y plane (perpendicular to build direction) and on the z plane (parallel to build direction) could be examined. Two types of test samples were fabricated of each of the alloy materials: (1) 1cm x 2cmx1cm metallurgical sample for microstructure characterization and (2) cylindrical 0.5" diameter x 3" long mechanical test specimens to determine mechanical properties. Of the materials procured to build the test coupons, QCML had prior experience with part fabrication using Alloy 718. However, initial experimentation to define build parameters was necessary for both Alloy 600 and Alloy 800.

Table 6 shows the process conditions used for the Inconel 600 metallurgical samples build and Figure 8 shows layout for the Inconel 600 fabrication, as well as the resulting metallurgical test samples. Several process conditions were used to determine what parameters most affected the quality of the sample. The density was used to determine which samples would be selected for microstructure examination. The samples with the density closest to the literature would be used. The process parameters had an effect on the fabricated part density. Figure 9 shows the variation

of density with laser power and laser scan speed. From the data, at a laser power of 195W, the Inconel 600 samples were generally insensitive to laser scan speed. The range of densities at 195W was 8.36 to 8.38g/cm^3 with a standard deviation of 0.013. The trends are consistent with the expectation that lower laser powers and higher scan speeds have a negative impact on sample density.

Table 6. Table Showing Process Trial Conditions and Parameters Matrix for Metallurgical Samples

	Specimen size	Scan speed	Laser power			
Inconel 600	1cmX2cmX1cm	1100mm/s	195W		Standard EOS	
Inconle 718	1cmX2cmX1cm	1200mm/s	195W		Standard EOS	
	1cmX2cmX1cm	1000mm/s	195W	180W	165W	150W
	1cmX2cmX1cm	900mm/s	195W	180W	165W	150W
	1cmX2cmX1cm	800mm/s	195W	180W	165W	150W
	1cmX2cmX1cm	1200mm/s	195W	180W	165W	150W
	1cmX2cmX1cm	1400mm/s	195W	180W	165W	150W

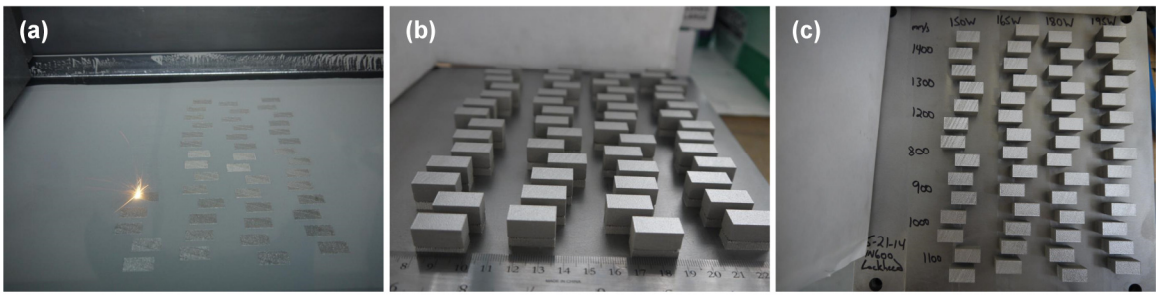

Figure 8. Pictures showing (a) the layout for the process trial matrix, (b) sample specimens fabricated, (c) all of the specimens with the scan speed listed.

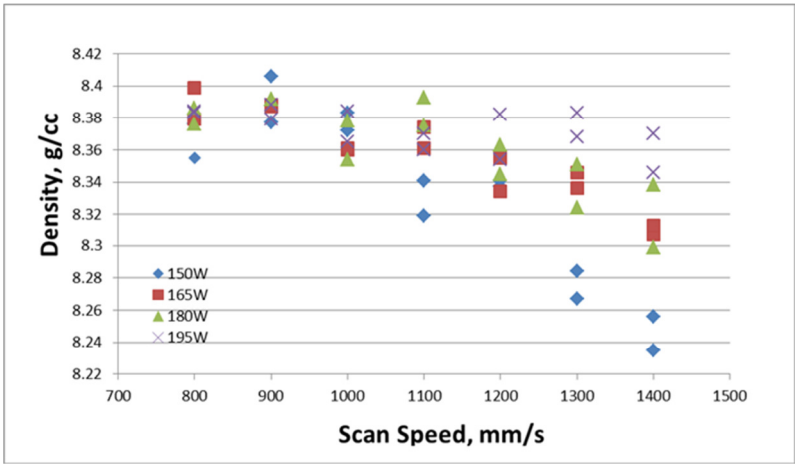

Figure 9. Graph showing effect of scan speed and laser power on fabricated Inconel 600 part density. At a laser power of 195W, the sample density is nearly insensitive to scan speed ranging from 8.35 g/cm^3 to 8.39 g/cm^3.

In total 56 (1cm x 2cm x 1cm) Inconel samples were built in the process trial matrix. Fourteen of which were selected for shipment to LM Advanced Technology Center (ATC) for further microstructure characterization and analysis. Based on the process trials the mechanical test coupons were built using 195W laser power and a scan speed of 1100 mm/s the process parameters.

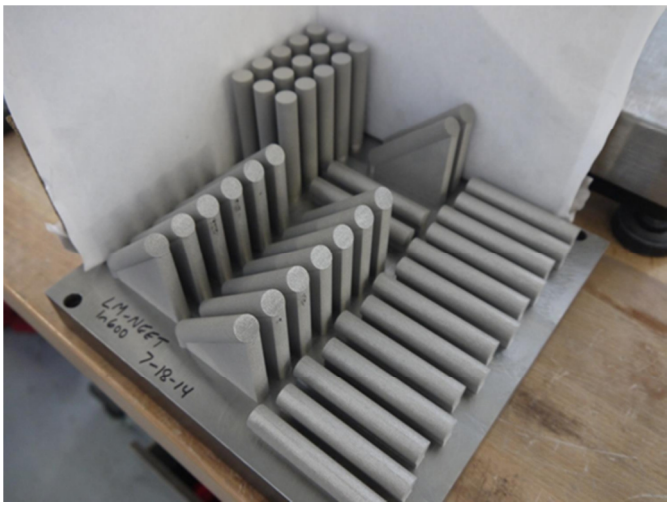

Figure 10. Inconel 600 longitudinal, transverse, and 45° specimens after LDM; samples were heat treated @ 900C for 1hr in Argon

This build layout produced 45 test coupons in a single build and is the maximum number that can be produced in a single build on the available build platform. The test coupons are cylinders with 0.5" diameter by 3" length. 15 cylinders are in horizontal orientation, 15 cylinders are in vertical orientation and 15 cylinders are at 45 degrees with respect to the horizontal. The process trial matrix used for the Inconel 600 samples was the same one used for the Inconel 718 and the Incoloy 800 process trial matrices. Figure 10 shows the Inconel 600 build mechanical test samples.

The details of the process variation consisted of four different Powers (W) used: 150, 165, 185, 195 Watts, seven different speeds (mm/s) were used: 800, 900, 1000, 1100, 1200, 1300, 1400 (mm/s) in increments of 100 from 800-1400. The crystal structure listed in the summary is that of the dominant constituent and the density listed is based on average densities for each of the power settings. A summary of results from the process parameter variation study can be found in Table 7.

Table 7. Results from Process Parameter Variation Study

	Inconel 600	**Inconel 718**	**Incoloy 800**
Chemical composition (%)	*72* **Ni**, *14-17* **Cr**, *6-10* **Fe**, *0.15 max* **C**, *1 max* **Mn**, *0.015* **S**, *0.50* **Si**, *0.50* **Cu**	*50-55* **Ni**, *17-21* **Cr**, *11-22.5* **Fe**, *0.08 max* **C**, *0.35* **Mn**, *0.015* **S**, *0.35* **Si**, *0.3* **Cu**, *0.2-0.5* **Al**, *0.65-1.15* **Ti**, *0.015* **P**, *1* **Co**, *4.75-5.5* **Nb**, *0.006* **B**, *2.8-3.3* **Mo**	*30-35* **Ni**, *19-23* **Cr**, *39.5 min* **Fe**, *0.1* max **C**, *0.8 max* **MN**, *0.008 max* **Si**, *0.4* **Cu**, *0.15-0.60* **Al**, *0.15-0.60* **Ti**,
Melting point (F)	2470-2575° F	2300-2435°F	2471-2525°F
Density (g/cm^3)	8.47	8.19	7.94
Crystal structure*	FCC	FCC	BCC or FCC
Process parameter study conditions: Power (W)	150 - 195	150 - 195	150 - 195
Process parameter study conditions: Scan Speed (mm/s) in increments of 100	800-1400	800-1400	800-1400
Density (g/cm^3) data range results:	8.29-8.39	8.11-8.20	7.80-7.91
Test coupon build conditions:	195 W, 1100 mm/s	195W, 1200mm/s	195W, 1200mm/s

The final test coupons for mechanical testing and characterization can be seen in Figure 11 for the remaining materials Inconel 718, Incoloy 800, and the 316L SS. The Inconel 718 samples were heat treated similarly as the Inconel 600 samples at 900C for 1hr in Argon, the Incoloy 800 samples were not heat treated, and the 316L SS samples were heat treated at 650C for 1hr in Argon.

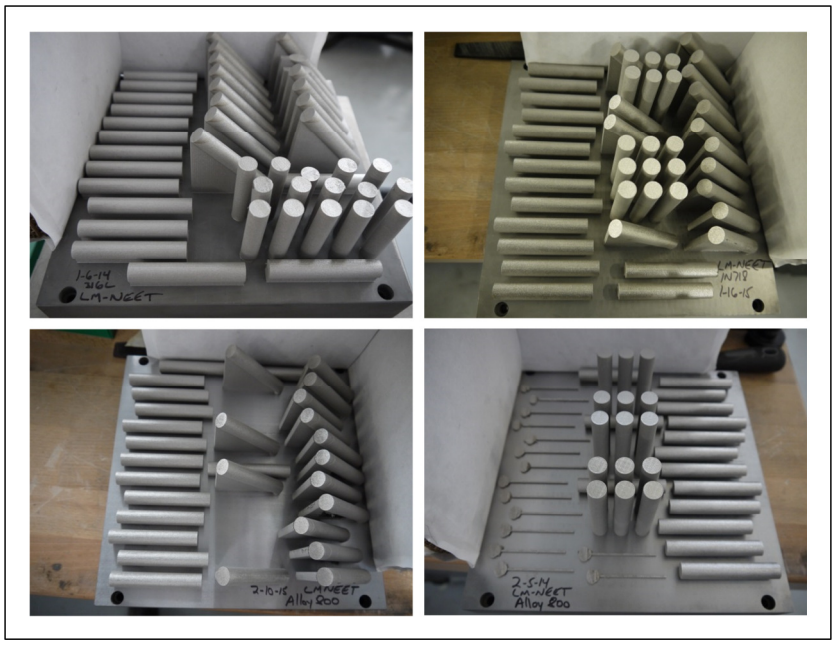

Figure 11. Top Left: 316L SS samples, top right: Inconel 718 samples, bottom left: Alloy 800 horizontal and 45 degree samples and bottom right: Alloy 800 vertical samples

While the Inconel / Incoloy and 316L metal powders were procured, the Oxide Dispersed Steel (ODS) powders were not. Typically ODS powders are made by mechanical milling of the oxide into the ferritic alloy. The ODS powders are not readily available for procurement. Three methods of obtaining the ODS powders were identified: (i) GARS- gas atomization reaction synthesis; (ii) Spray Drying; and (iii) Ball Milling.

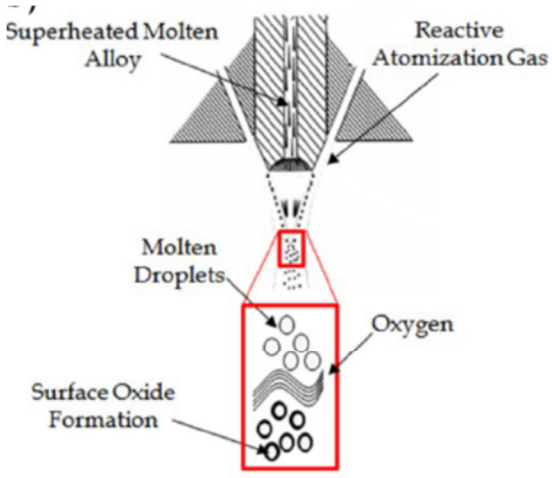

Figure 12. Sketch of GARS process

The GARS method was developed by Dr. Iver Anderson out of Ames Laboratory. His method uses warrants a brief discussion as it has the potential for success using the DMLS technique. The method is a gas atomization reaction synthesis (GARS) process and is illustrated in Figure 12. The process uses a reactive atomized gas and the rapid solidification process of the molten metal which produces particles with a thin surface layer of oxide, forming a metastable oxide phase. At high temperature, initial consolidation results in oxide at particle boundaries; this dissociates releasing oxygen for formation of yttrium containing oxide dispersoids.[8] Due to budget constraints this

was not a feasible path for the program.

The focus of procuring a ready-made ODS powder returned to acquiring the components for a mechanical type of process. An attempt was made to use a different type of mechanical process from the mechanical milling. Flurry Powders, LLC was identified as company that could make metal powder materials via a spray drying technique. They use a spray drying process that requires wet blending for blend uniformity. The liquid feed then is atomized into the spray dryer. The dried droplets naturally form flow-able steel-oxide spheres of blend uniformity comparable to the wet formulation. By varying the wet formulation and spray parameters the process is able to control particle size. This process relies heavily on having the correct binder/component formulation to produce the powder of interest. Several trials were completed without translating into the required ODS material formulation.

A mechanical milling process was used to produce the ODS powder for process trials and fabrication of metallurgical samples. The ODS powder was made at the ATC from the individual constituents (316L SS, 44 to 105 um particle size and Yttria 40nm particle size) and then ball milled to create a dispersed powder shown in Figure 13a. The ball milling procedure uses the constituent materials (316L SS 40-104 um particle size and Yttria <50nm particle size) and a milling media (1/2"' diameter, cylindrical alumina). It was milled for approximately 24 hours and then initially screened (2mm) to remove the media followed by a second screening 120 mesh (125 um)to remove large agglomerates The process yielded approximately 22 pounds of ODS powder to use with QCML's beam deposition system.

QCML was able to make the metallurgical samples shown in Figure 13b of the ODS powder alloys. QCML used their beam deposition system (DED/LENS) which requires less starting material than the powder bed system. With this system powder is delivered through the nozzle that also houses the laser hence beam deposition. The parameters used in the first three trials are listed in Table 8.

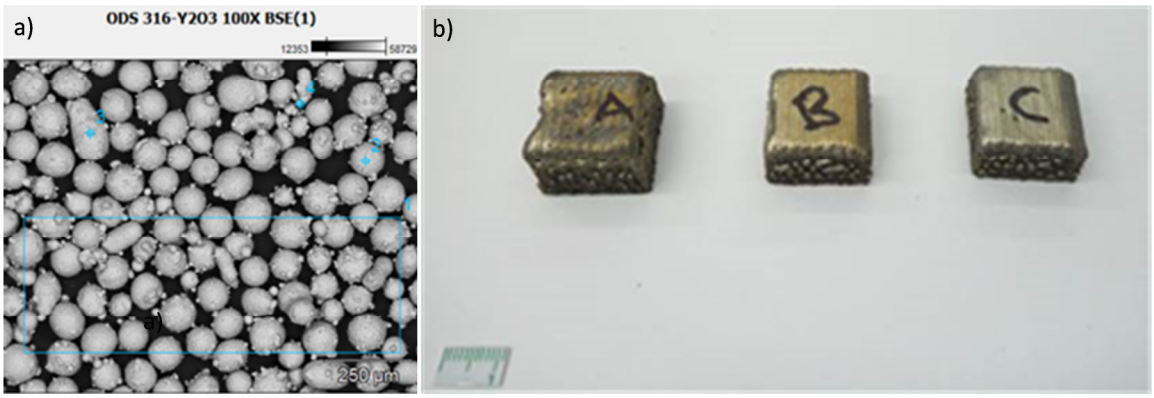

Figure 13. Oxide dispersed strengthened material development: (a) ODS Steel (316L SS 44-105um) and Yttria ball milled powder; (b) ODS process trial metallurgical samples.

Table 8. Initial ODS Trials Using LENS System

Process Parameters	A	B	C
Speed (mm/s)	15	12.7	15
Slicer Vertical Distance (mm)	0.25	0.43	0.43
Slicer Horizontal Distance (mm)	0.9	1.07	1.07
O2 (ppm)	under 50	under 50	under 50
Power (W)	870 (7.8)	780 (7.0)	780 (7.0)
Powder feeder setting	7	6	6
Powder (g/min)	pending	pending	pending

The metallurgical samples were examined for porosity to help optimize the parameters of the next build. Figure 14 shows the un-etched and etched versions of the metallurgical samples. Based on initial microstructure data and density sample "A" parameters will be used to build tensile specimens. While sample "A" is not ideal as it has more porosity than it should, it is a good starting point. Its density of 7.862 g/cm^3 is the closest to that of 316L SS 7.99g/cm^3.

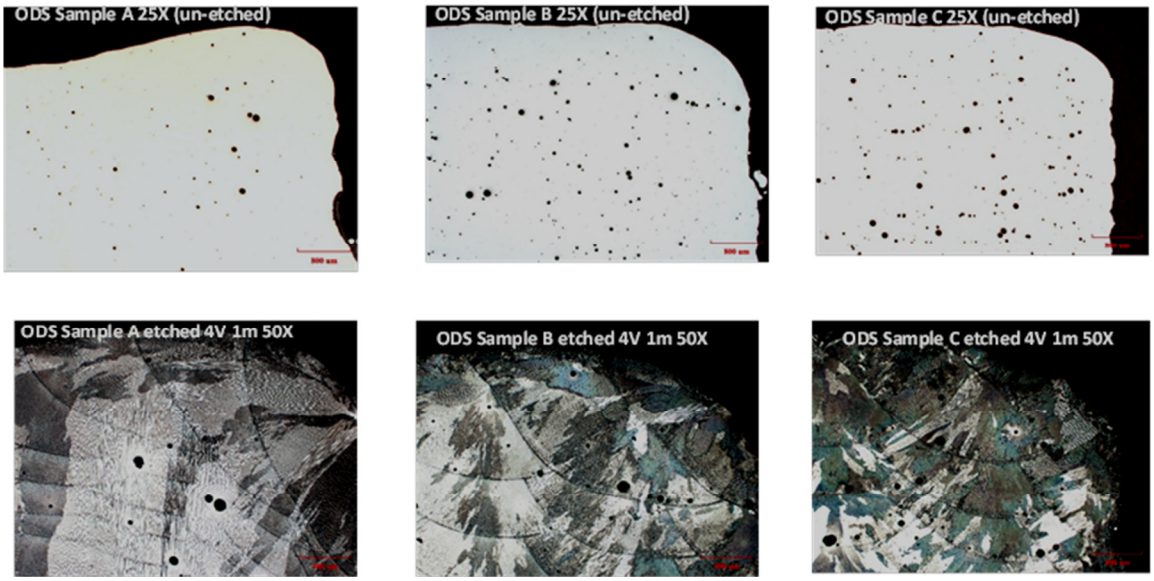

Figure 14. ODS Steel Images of the etched and un-etched microstructures. Top row: L->R Un-etched samples A-C showing porosity of each, Bottom row: L->R etched samples A-C showing the fine microstructure and melt pools.

The AM technique lends itself well to the types of complex components that are needed in a nuclear reactor. The articles need less post machining and can be heat treated post manufacturing, if material requires. This type of manufacturing can also lead to tailoring of the microstructure as well as use novel materials otherwise not used in industry. By fabricating these articles demonstrates the ability to take a complex design and fabricate it with little post processing.

3.2.3 Evaluation and Characterization of Test Articles

It is critical to understand the process-structure-property relationships in order to optimize and improve performance of most materials. In this study the process selected deviated from the traditional modes of manufacturing with austenite nickel-chromium-based alloys and 300 series stainless steels. A full set of data was collected for the Inconel 600 samples as well as the 316L samples. A correlation between the microstructure and mechanical properties will be presented with the information collected.

The test coupons built with DMLS process were characterized by Scanning Electron Microscopy (SEM), Energy Dispersive Spectroscopy (EDS) and Optical Imaging for microstructure determination and tensile testing (ASTM E8) to characterize the mechanical properties. Vickers Hardness test was used to characterize the hardness and correlated to a Rockwell B hardness value that is reported in literature. Five test coupons of each material in the three build orientations were sent to LM for evaluation. Three samples from each build orientation (nine samples) per material (Inconel 600 and 316L) were tested to gather statistical deviation in characterized properties.

All 18 samples were machined to the ASTM E8/E8M standard. The machining process can be seen in Figure 15. The samples were then tested at LM B/195b test labs with a calibrated Instron 4505 with an Instron 1" extensometer with a crosshead rate of 0.05"/minute. The measurement uncertainty for the load, stress and elongation is approximately 1%. The samples were not threaded as the Instron has clamps that make threading the samples unnecessary.

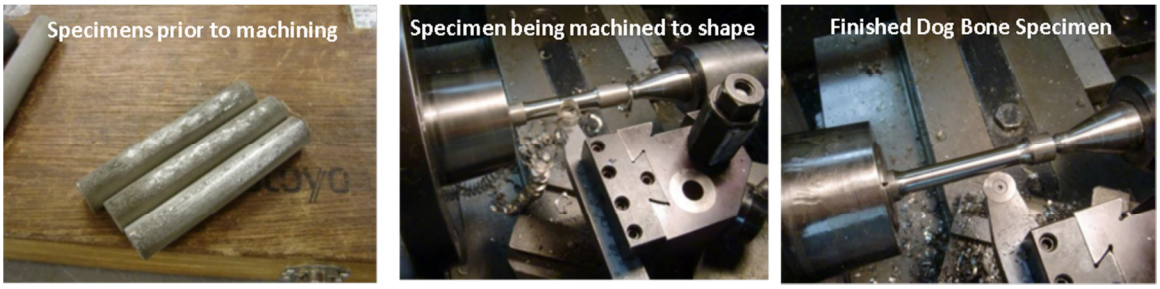

Figure 15. Machining of Inconel 600 samples to the standard test methods for tension testing of metallic materials—ASTM E8/E8M.

Case Study 1: Inconel 600

From the load extension curve Figure 16, it is apparent that the directionality of manufacturing has an impact on the maximum tensile strength. The vertical (z-axis) direction had the lower tensile strength which is the build direction.

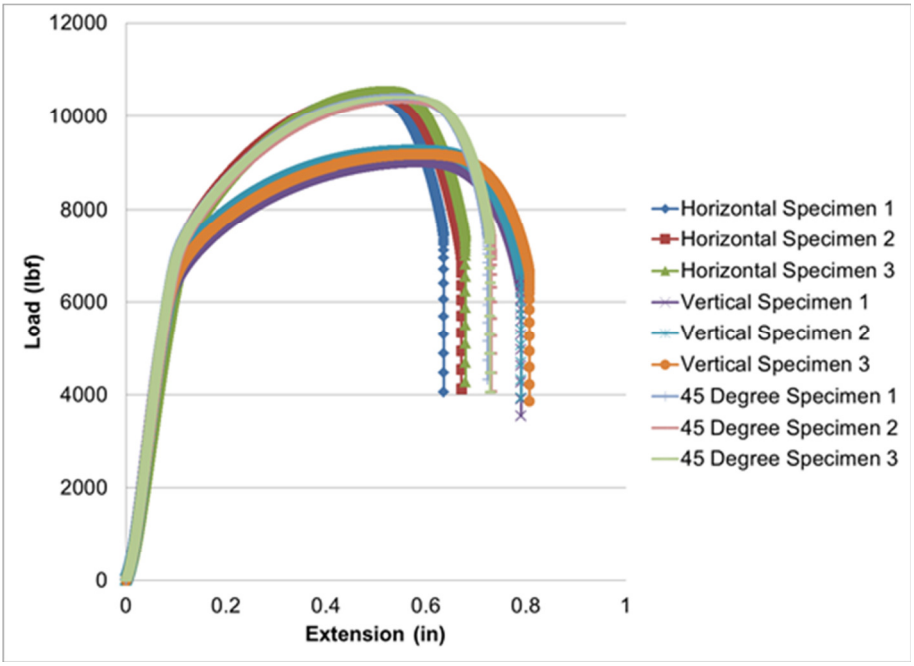

Figure 16. Load-Extension Curves for Inconel 600 Samples Manufactured in the three orientations: horizontal, vertical, and 45 degrees.

The resulting test data shows properties comparable to the Inconel 600 rod/ bar stock which is summarized below in Table 9. Although, the directionality of the build has an impact the DMLS manufactured samples mechanical properties are comparable to properties found in the literature.

Table 9. Comparison of Inconel 600 Bar/Rod Stock to Direct Manufactured Samples

Inconel 600	Maximum Load [lbf]	Yield Stress (Offset 0.2 %) [ksi]	Max Tensile Strength [ksi]	Modulus (0.05-0.01%) [ksi]	Elongation [%]	Reduction of Area [%]
Cold-drawn Annealed *from literature*	-	25-50	80-100	-	55-35	-
Cold-drawn As-drawn *from literature*	-	80-125	105-150	-	30-10	-
Hot finished Annealed *from literature*	-	30-50	80-100	-	55-35	-
Hot Finished Hot-finished *from literature*	-	35-90	85-120	-	50-30	-
Horizontal Mean of all three *Direct Manufactured* specimens	10,458	70.9	105.3	30,110	39	65
Vertical Mean of all three *Direct Manufactured* specimens	9,158	64.6	92.2	30,057	49	69
45 degree Mean of all three *Direct Manufactured* specimens	10,376	70.3	104.3	33,633	43	64

Following the tensile tests fracture surface analysis was completed on the samples. SEM, EDS and Optical Imaging were used to examine the fracture surface of three tensile from each material set. One tensile specimen from a vertical, horizontal and 45-degree orientation was examined. The material composition was measured using EDS and was found to be consistent with Inconel 600 specifications. No titanium nitride particles were detected in any of the fractures examined. Titanium nitrides are common in traditional Inconel 600 which solidifies more slowly than direct-manufactured material.

All nine tensile samples exhibited ductile cup-and-cone fracture which includes shear lips. This is indicative of ductility. Images of the samples for the Inconel 600 are shown in Figure 17. The fracture surface analysis showed that ductile cup-and-cone fracture was present in all samples examined see Figure 18. The voids were likely produced during direct manufacture and were enlarged by the plastic flow which occurred during tensile testing.

Figure 17. All nine Inconel 600 Samples after Tensile Testing

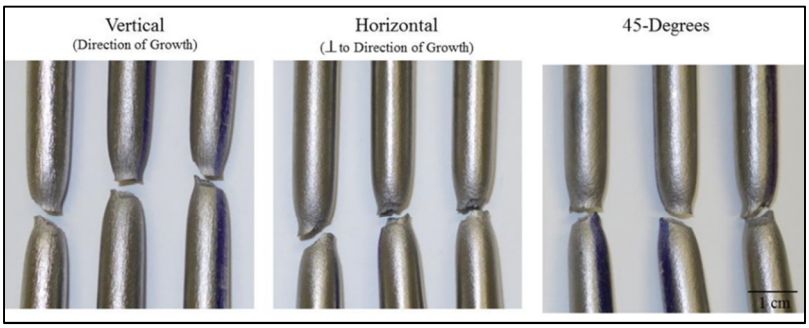

Figure 18. All nine samples show ductile cup-and-cone fracture

The 45-degree samples had a slight "chiseled" appearance when compared to the vertical and horizontal samples when viewed optically as seen in Figure 19. Stating that difference it appears they all failed similarly and that the manufacturing orientation was not a factor in the type of fracture.

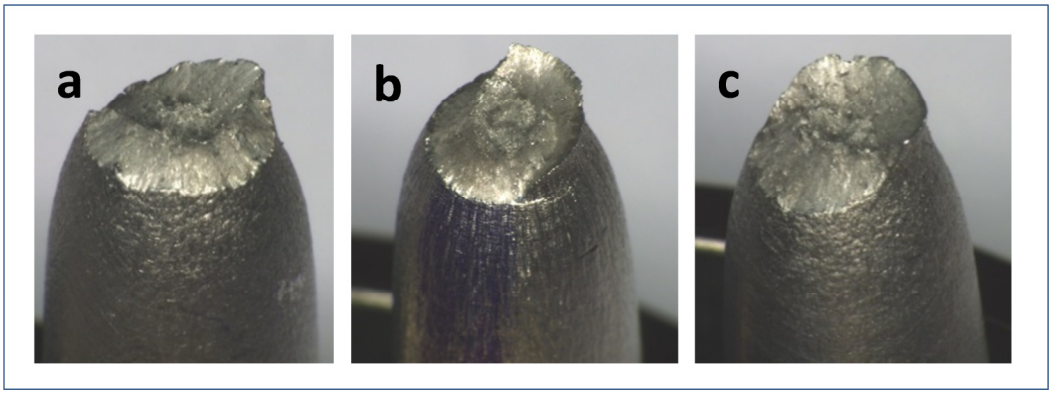

Figure 19. (a) 45-degree optical image showing "chiseled" appearance compared to (b) vertical sample and (c) horizontal sample

Shear ductile dimples are seen in both the shear lip of the cup and cone as well as in the center fracture, in each of the manufactured orientations. Images of the ductile dimples can be seen in Figure 20(a), (b) and (c) for the cup section of vertical sample V-1 and Figure 21(a), (b), and (c) show the ductile dimples for the cone section of the same vertical sample V-1. Voids were also present and visible as dark areas that have been enlarged by tensile testing.

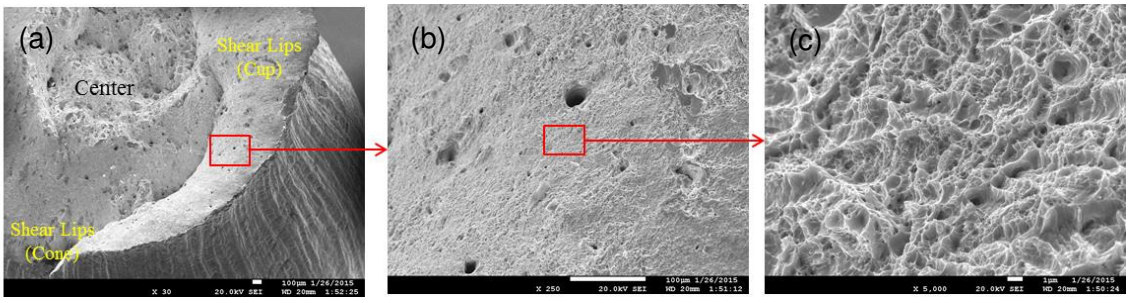

Figure 20. Ductile Dimples of the cup section from the Inconel 600 of vertical build sample

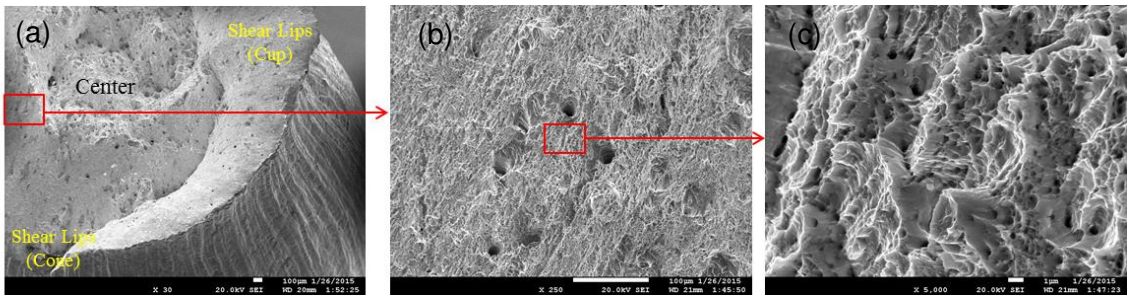

Figure 21. Ductile Dimples of the cone section from the Inconel 600 of vertical build sample

Of the 56 Inconel 600 metallurgical samples QCML fabricated, fourteen were selected and shipped to the ATC for further down selection. From the fourteen, five of the samples were selected for microstructure characterization. Backscattered electron imaging was used to look at the microstructure of bar stock Inconel 600 and the DMLS manufactured Inconel 600 sample.

Noticeable grain structure differences are seen due to the manufacturing process in Figure 22 and Figure 23.

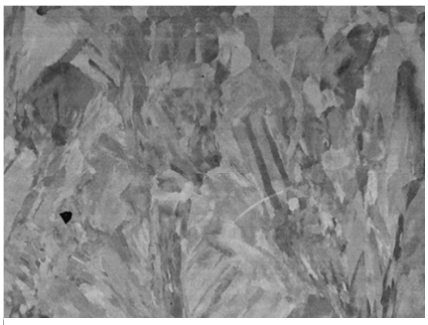

Figure 22. DMLS manufactured Inconel 600 Sample; 500X BSE 10kV not etched

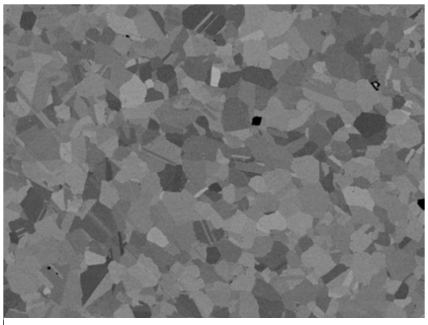

Figure 23. Inconel 600: Bar Stock Sample; 500X BSE 10kV not etched

In section 3.2.2, it was noted that at a laser power of 195W, the Inconel 600 sample density is generally insensitive to the scan speed making for a stable process. Table 10 provides a summary of the microstructure analysis of the five samples examined. Sample #12 was sectioned for mounting in both the x-y & z directions for a total of five samples, examined with one sample examined from two directions. Each sample went through the sample metallography procedure which included: Mounting, grinding, polishing, micrograph collection (photographs), Scanning Electron Microscopy (SEM), etching, a second micrograph, and a final SEM imaging. From the micrographs, representative sample voiding is visible indicating that the samples produced at the higher speed rate and lower power contain more voiding.

Table 10. Summary of five samples selected for microstructure examination

Sample #	Sample name	Micrograph (100X)	Density (g/cm3)	Proces Parameters		Notes:
				Power (W)	Speed (mm/s)	
4	600_150_1400	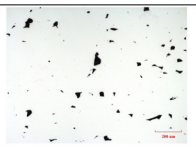	8.235	150	1400	
10	600_180_1400		8.299	180	1400	
11	600_195_800		8.384	195	800	
12 (a)	600_195_1100		8.37	195	1100	Sample #12 was selected to be mounted in both the x-y & Z planes (long)
12 (b)	600_195_1100		8.37	195	1100	Sample #12 was selected to be mounted in both the x-y & Z planes (trans)
14	600_195_1400		8.346	195	1400	

As part of the overall microstructure evaluation of the test samples, the edge transition s at initiation and termination were examined along the vertical build axis (Figure 24). An Oxalic acid (HOOCCOOH) etch was used to help delineate the microstructure at each location. It was found that the initiating layer of the build the microstructure has an equiaxed grain structure. As the specimen transitioned from the initiating layers a more elongated grain structure was seen (Figure 25)

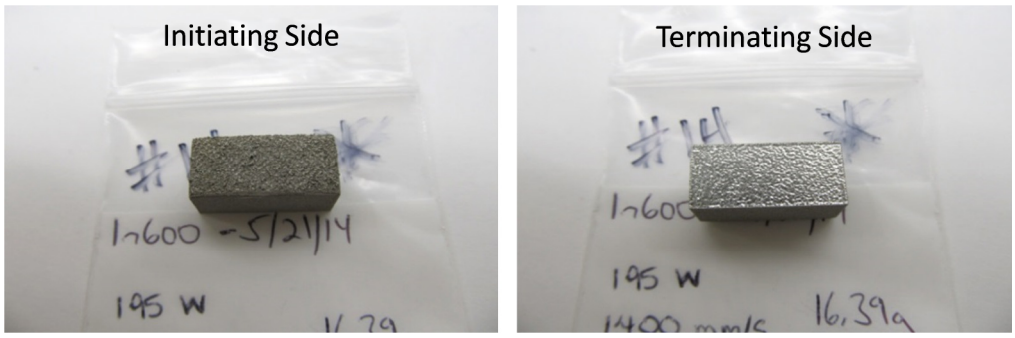

Figure 24. Photographs of Inconel 600 Sample 600-195-1400 (1cm x2cmx1cm) initiating and terminating sides of build.

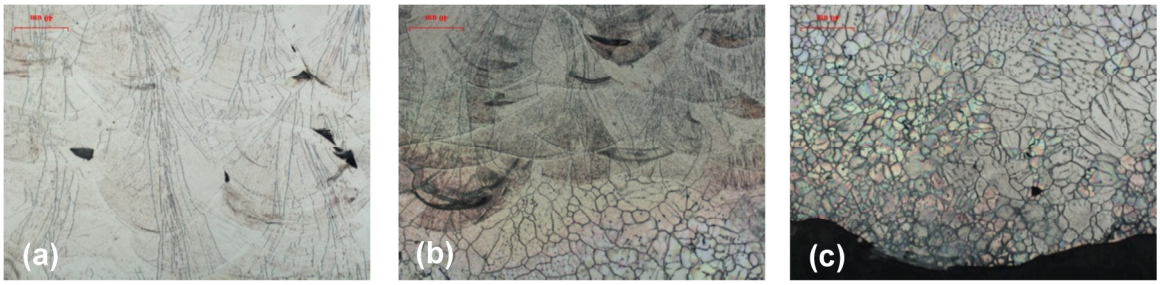

Figure 25. Micrographs of Etched Sample #14 showing Edge transitions at 500X: (a) top of sample away from initiating side, (b) transition, (c) initiating edge at the bottom of sample.

Inconel alloy 600 is a stable, austenitic solid-solution alloy. The only precipitated phases present in the microstructure are titanium nitrides, titanium carbides (or solutions of those two compounds commonly called cyanonitrides), and chromium carbides. Titanium nitrides and carbides are visible in polished microspecimens at magnifications of 50X or greater. They appear as small, randomly dispersed, angular-shaped inclusions. The color varies from orange-yellow for the nitride to gray-lavender for the carbide. These nitrides and cyanonitrides are stable at all temperatures below the melting point and are unaffected by heat treatment. At temperatures between 1000° and 1800°F (540° and 980°C), chromium carbides precipitate out of the solid solution. Precipitation occurs both at the grain boundaries and in the matrix. Because of the grain-boundary precipitation, the corrosion behavior of Inconel alloy 600 is similar to that of other austenitic alloys in that the material can be made susceptible to inter-granular attack in some aggressive media (sensitized) by exposure to temperatures of 1000°F to 1400°F (540C to 760C). At temperatures above 1400°F (760C), the predominant carbide is Cr7C3. Below 1400°F (760C), the Cr23C6 carbide is also present.

Backscattered electron imaging of sample 600-195-1400 (sample #14) revealed the solidification/grain microstructure. The microstructure appeared similar in the three locations examined. No titanium nitride particles were detected (titanium nitride particles are typically found in wrought material). The black areas in images are voids in Figure 26.

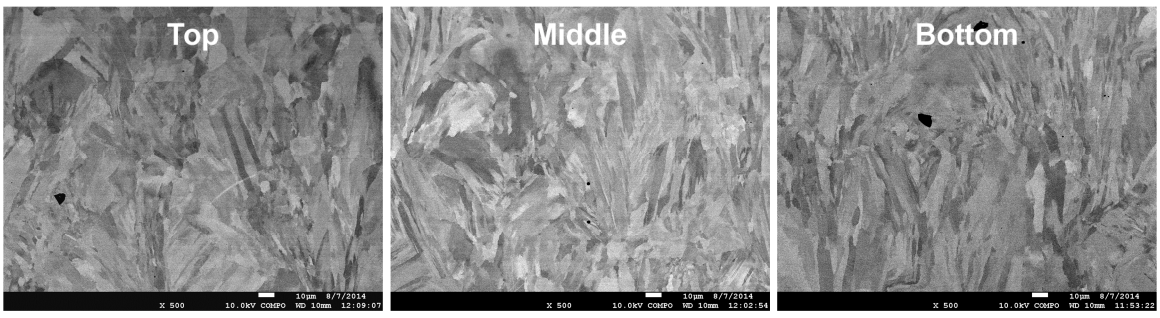

Figure 26. Backscattered Electron Imaging of Sample 600-195-1400 in three locations; No titanium nitride particles present; Dark irregular shaped spots are voids in the material.

The microstructure of the XZ and XY planes of sample 600-195-100 (sample #12) were examined both with optical imaging, shown in Figure 27, and SEM analysis, shown in Figure 28. The SEM images of the un-etched mounts for the XZ and XY planes show sub-grain structure and the etched XY plane shows the laser solidification structure of the sample.

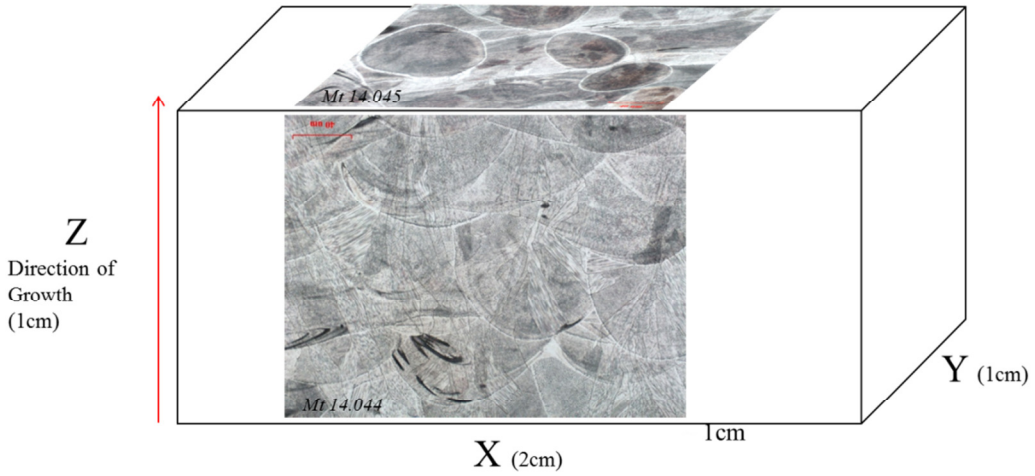

Figure 27. Optical images of the etched Inconel 600 Sample 600-195-1100 (sample #12); laser solidification patters for both XZ and XY planes (note the optical images are scaled substantially higher than the XYZ dimensions of the specimen); sample etch: electrolytic oxalic acid, 4V for 10 sec.

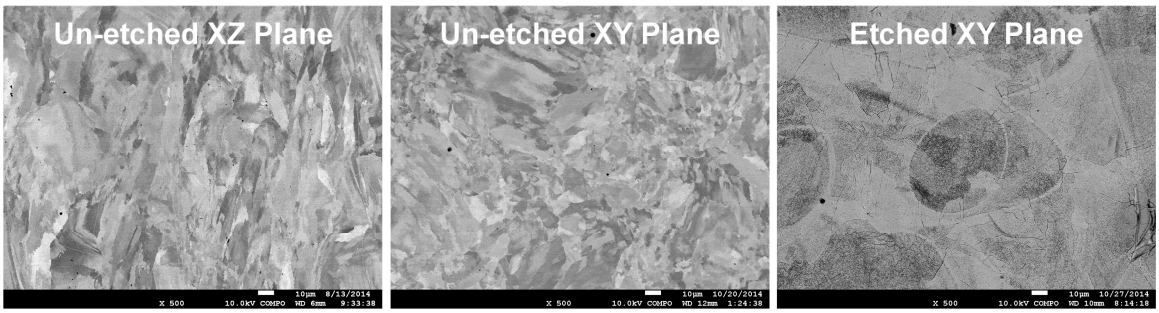

Figure 28. SEM images showing the sub-grain structure of the un-etched XZ and XY planes and the solidification structure of the XY etched plane.

The solidification texturing seen in the micrographs and the tensile data lead to doing preliminary investigation of a preferred orientation in the build direction. Preliminary XRD data shows the differences in peak ratios between the horizontally and vertically built specimens in Figure 29. This data supports the directional solidification texturing seen in the micrographs.

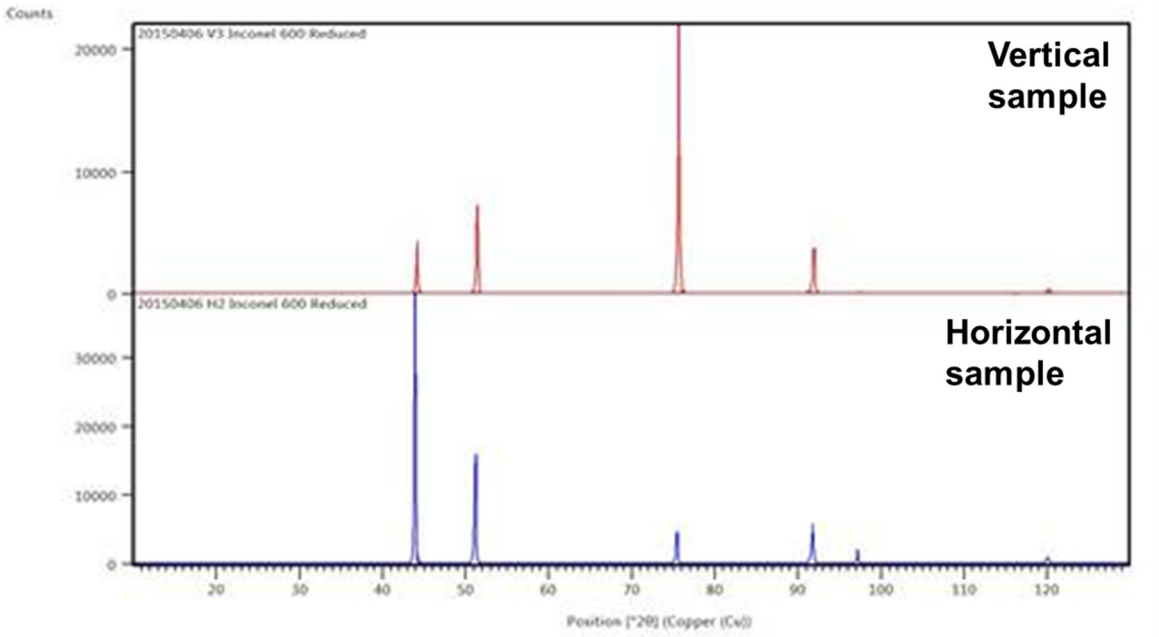

Figure 29. XRD showing peak ratio differences in the vertical and horizontal build directions

Optical images of etched DMLS manufactured Inconel 600 material show microstructure for both XZ and XY planes in both non-heat treated and heat treated conditions and are shown in Figure 30. The laser 'pools' are evident in the sample with no heat treatment but not as evident in the heat treated sample. The grains appear more elongated in the heat treated microstructure which would be indicative of a stress relief heat treatment.

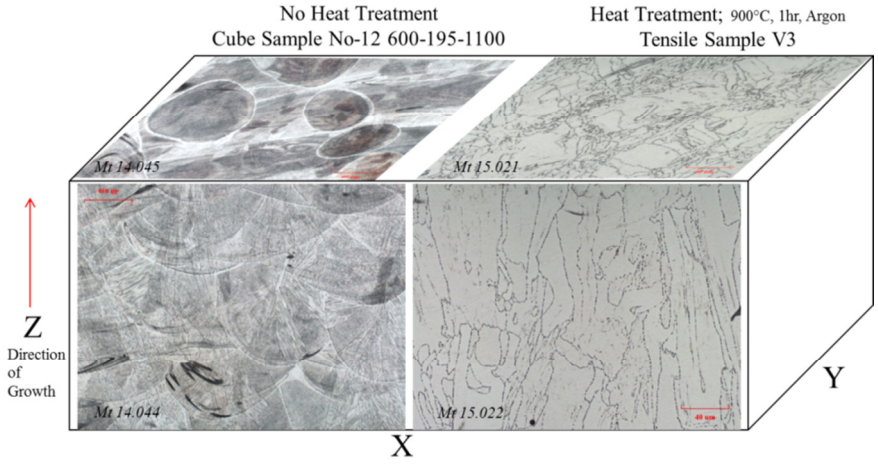

Figure 30. Optical images of the etched Inconel 600 non heat treated vs. heat treated.

A summary of the Inconel 600 case study showed that the properties of the DMLS Inconel 600 samples are in alignment with that of the wrought bar stock Inconel 600. The mechanical testing of the DMLS fabricated samples (before heat treatment) showed directional dependence. The fracture surface analysis showed that ductile cup-and-cone fracture was present. The

microstructure examination showed the directionality and solidification patterns for this type of process on Inconel 600 and that there is likely a preferred orientation for this material in the build direction.

Case Study 2: 316L Stainless Steel

These 316L SS tensile samples were heat treated at 650C for 1hr in Argon. This is a typical stress relief heat treatment. The 316L SS samples were tensile tested at room temperature in the same 195B laboratories as the Inconel 600 samples. The results were similarly compared to rod or bar form cold-drawn annealed and hot finished 316L SS properties. The data from the tensile test should provide tensile strength, yield strength (0.2% offset), reduction of area, and percent (%) elongation, which is provided in Table 11 for 316L SS. All samples were tested with the Instron 4505 with a crosshead rate of 0.05"/minute. The measurement uncertainty for the load, stress and elongation is approximately 1%.

From the load extension curve Figure 31, the data reinforces that the directionality of manufacturing has an impact on the maximum tensile strength, as was noted with the Inconel 600 samples. The vertical (z-axis) direction had the lower tensile strength than the other two build orientations.

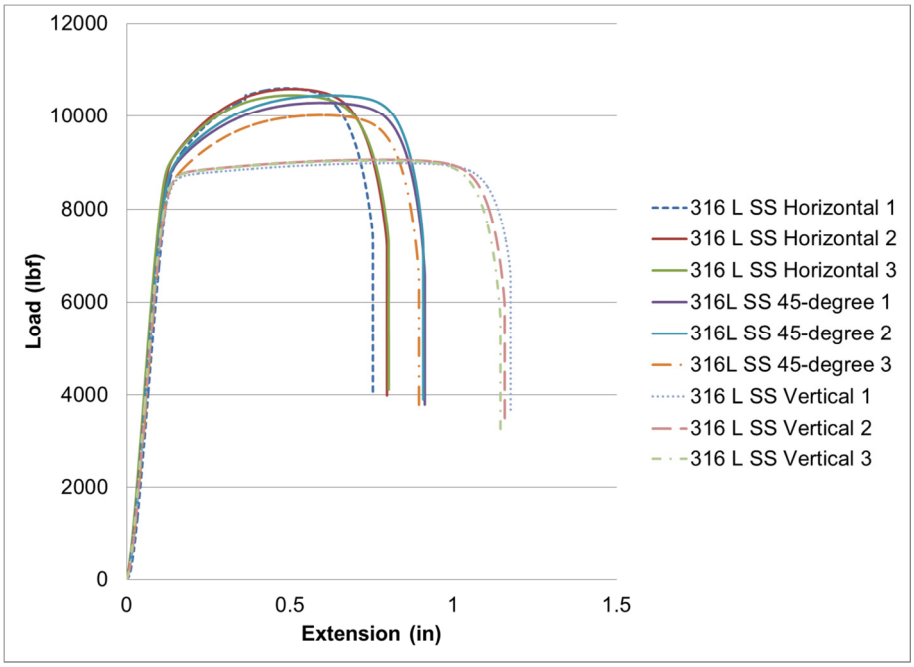

Figure 31. Load-Extension Curves for 316L SS samples manufactured in the three orientations: horizontal, vertical, and 45 degrees.

Table 11. Comparison of 316L SS Bar/Rod Stock to Direct Manufactured Samples.

Type	Maximum Load [lbf]	Yield Stress (Offset 0.2 %)[ksi]	Max Tensile Strength [ksi]	Elongation [%]
316L* *from literature*	-	42	81	50
Horizontal Mean of all three *Direct Manufactured* 316L SS specimens	10,552	90.4	111.0	48.7
45 degree Mean of all three *Direct Manufactured* 316L SS specimens	10,254	87.6	108.4	57.3
Vertical Mean of all three Direct Manufactured 316L SS specimens	9,030	78.6	93.3	78

Following the same protocol as with the Inconel 600 specimen, SEM, EDS and optical Imaging were used to examine the fracture surface of three 316L SS tensile specimens. The tensile samples examined are indicated in Figure 32 by the red circle. The vertical samples were made in a separate additive manufacturing run than those in the horizontal and 45-degree samples. The vertical samples in original run did not reach sufficient height and were run at a later time. These are also indicated in Figure 32.

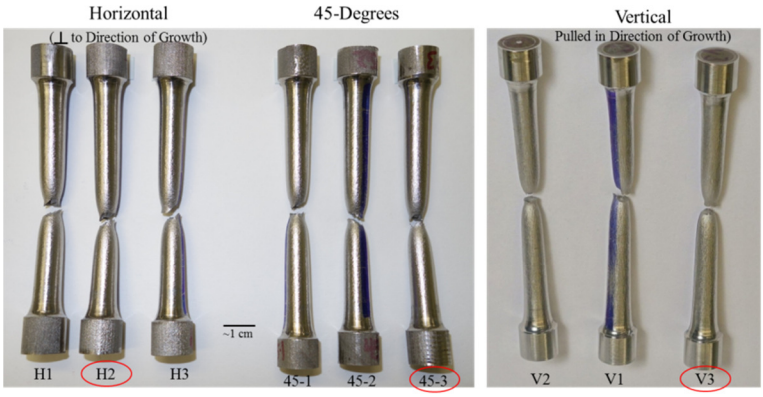

Figure 32. All nine 316L SS Samples after Tensile Testing.

All nine tensile samples exhibited ductile cup-and-cone fractures which include shear lips. The type of fracture is indicative of ductility. The material composition was measured using EDS and was found to be consistent with 316L specifications. Both the horizontal and 45-degree samples had a slight "chisel" appearance when viewed optically. Only one of the three vertical samples

had the “chisel” appearance. Ductile cup-and-cone fracture was present in all samples submitted example Figure 33. Direction of ductile dimples indicates a stress perpendicular to the direction of tension as seen in Figure 34 and Figure 35.

Voids that were likely produced during manufacturing process were enlarged by the plastic flow which occurred during tensile testing. In the vertical and 45 degree oriented samples the very large voids are associated with tears that can be seen in Figure 36 and Figure 37. There is a possible stress direction set up from presence of very large void.

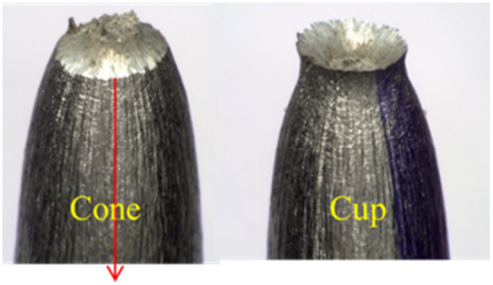

Figure 33. Cup- Cone fracture surface 316L SS vertical sample.

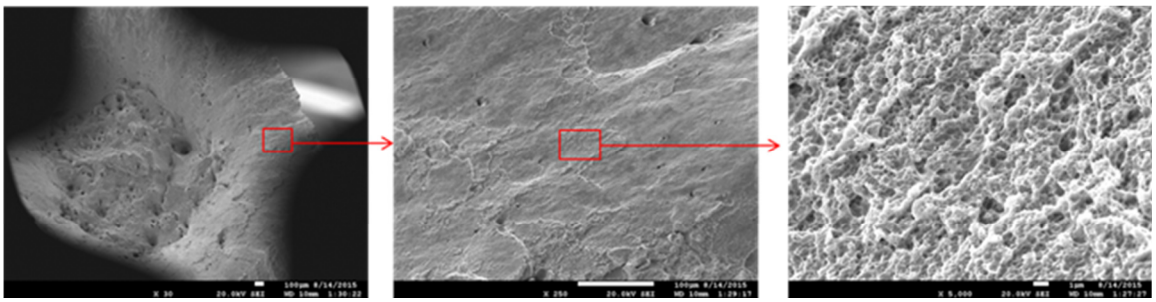

Figure 34. Ductile dimples of 316L SS vertical sample are shown in the shear lip (cup)

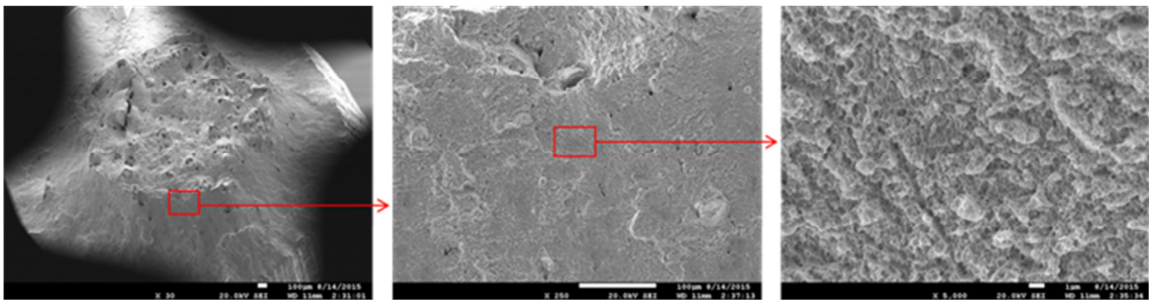

Figure 35. Ductile dimples of 316L SS vertical sample are shown in the shear lip (cone section)

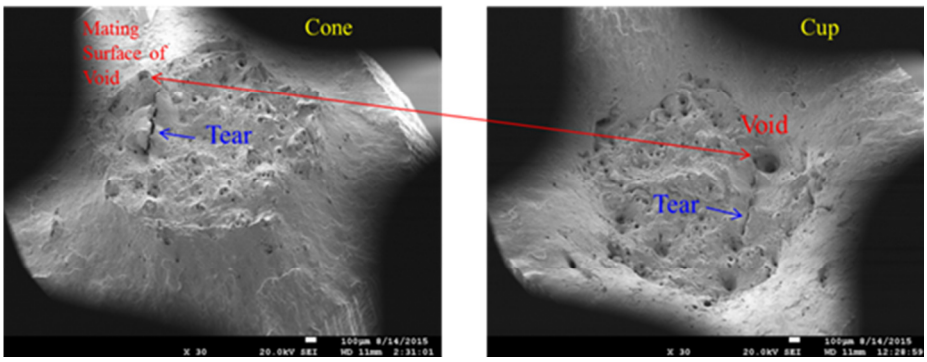

Figure 36. Vertical 316L SS sample mating surfaces of void are shown by red arrow and the tear in both surfaces.

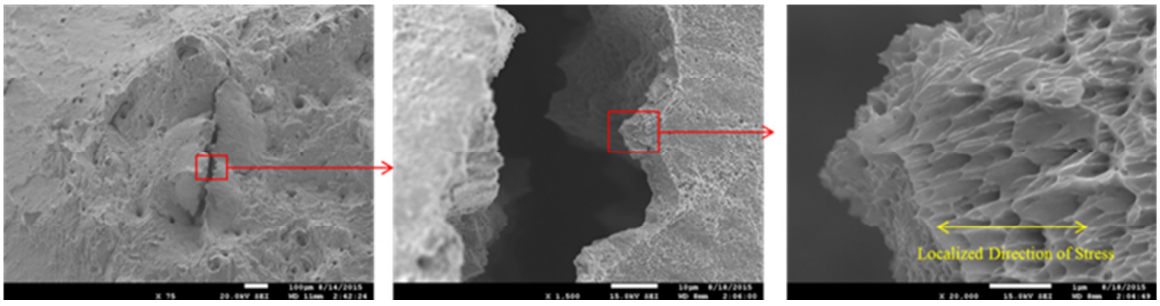

Figure 37. High-magnification images of a ductile tear within the fracture surface of the 316L SS sample

The fracture surface analysis for the 316L SS DMLS fabricated samples produced similar results as the Inconel 600. The fractured surfaces showed cup-cone ductile fractures. There was more evidence of tearing in the 316L SS samples than the Inconel 600 samples. This could possibly be due to the size of the voids in the316L SS samples. The pulled samples were cross-sectioned and polished for metallographic examination. Optical micrographs were taken both in the un-etched condition to show voids and in the etched condition to show microstructure. Figure 38 (a) shows the mounted fractured tensile specimen; and (b) shows evidence of voiding in the sample near the fracture surface.

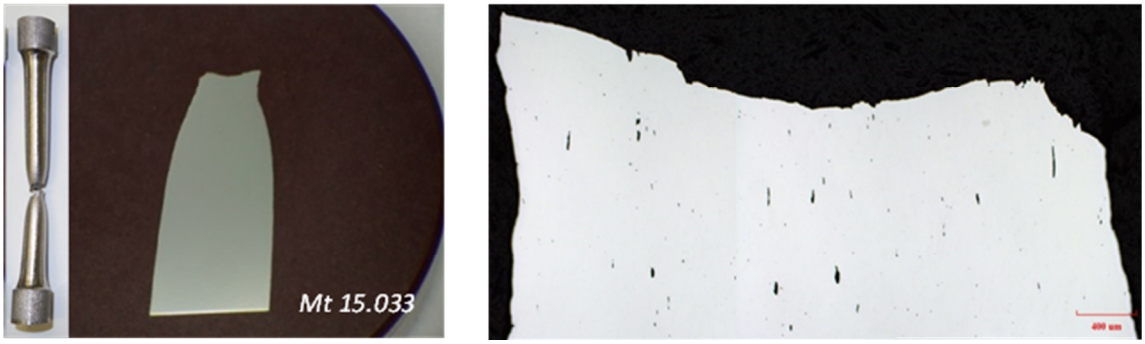

Figure 38. (a) 316L SS Horizontal Sample H2 and mount and (b) 316L SS Sample H2 shows the metallographic mount of the fracture surface of the lower half of sample

The voids are elongated in the necked area of the tensile sample. The necked area exhibits the most plastic deformation along the sample length. However, in an area approximately 1 cm from the necked region the voids are irregularly shaped but are not elongated as this region did not have the same amount of plastic deformation see Figure 39.

Figure 39. 316L SS Sample H2 micrograph of region ~1cm from necking, has irregularly shaped voids but not elongated

Optical images of etched sample H2 show microstructure for both XZ and XY planes. The laser melts 'pools' are evident in these samples as they were in the untreated Inconel 600samples. This is a difference from the heat treated Inconel 600 samples. The Inconel heat treated samples should less defined solidification patterning compared with the 316L SS heat treated sample seen in Figure 40.

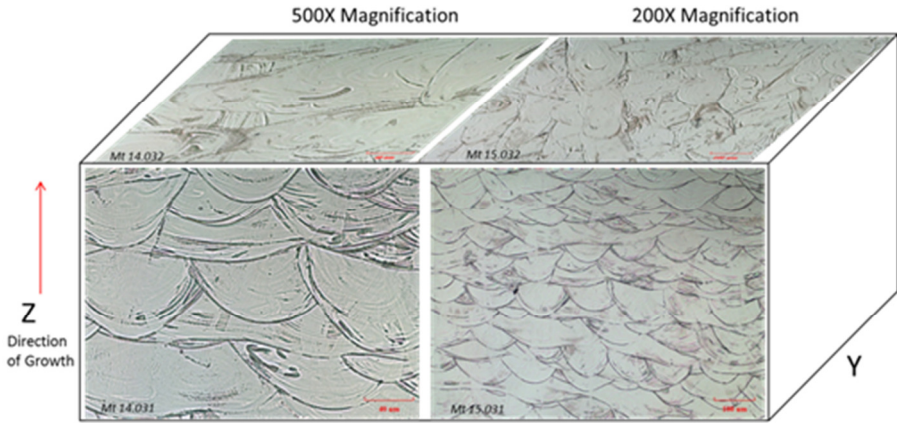

Figure 40. 316LSS Etched Sample H2 micrograph of microstructure in for both the XZ and XY Planes

The examination showed some voids are present throughout both horizontal (H2) and 45-degree (45-3) tensile samples. All of the voids have irregular (angled) surfaces. The voids are enlarged and elongated in the necked area near fracture which is consistent with observations made of fracture surface with the SEM. The grain shape reflects the laser solidification patterning

3.2.4 Discussion

In summary, the case studies show that the materials chosen for DMLS fabrication were compatible with the additive manufacturing process. The process worked well with both materials and process parameters were able to be optimized for each material. The materials yielded similar properties as the traditionally made materials. In the Inconel case the properties appeared to be slightly better than bar/rod stock Inconel 600. The 316L SS material had similar properties but

also exhibited lower tensile strength in vertical (Z) direction of growth. However, having this knowledge can be useful and factored into the design of parts. The set of techniques used for these case studies is what would be used to begin to characterize the materials and a new process. What has yet to be presented are the microstructure results from the additional heat treatment of the Inconel and 316L SS samples, the hot isostatic pressure process, and the results of irradiation testing that will be done at Texas A&M University. Schedule permitting the ODS material process parameters will be optimized to make tensile specimens and tested. The characterization completed was able to provide confidence in the feasibility of using DMLS for complex shapes with industry used materials. Further exploration of the preferential orientation of materials with this process could be another means to tailoring and controlling the microstructure using additive manufacturing.

3.2.5 References

[1] Y. Guerin, G. S. Was and S. J. Zinkle, "Materials Challenges for Advanced Nuclear Energy Systems," MRS Bulletin, vol. 34, pp. 10-18, 2009.

[2] T. Allen, J. Busby, R. Kluch, S. Maloy and M. Toloczko, "Cladding and Duct Materials for Advanced Nuclear Recylce Reactors," JOM, vol. 60, no. 1, pp. 15-23, 2008.

[3] T. Allen, H. Burlet, R. Nanstad, M. Samaras and S. Ukai, "Advanced Structural Materials and Cladding," MRS Bulletin, vol. 34, pp. 20-26, 2009.

[4] D. Biello, "Scientific American," 14 March 2011. [Online]. Available: http://www.scientificamerican.com/article.cfm?id=partial-meltdowns-hydrogen-explosions-at-fukushima-nuclear-power-plant.

[5] P. Olier, J. Malaplate, M. Mathon, D. H. D. Nunes, L. Toualbi, Y. de Carlan and L. Chaffron, "Chemical and microstructural evolution on ODS Fe–14CrWTi steel during manufacturing stages," Journal of Nuclear Materials, vol. 428, no. 1-3, pp. 40-46, 2012.

[6] S. Zinkle and N. Ghoniem, "Prospects for accelerated development of high performance structural materials," Journal of Nuclear Materials, vol. 417, pp. 2-8, 2011.

[7] X.-M. B. e. al., Science, vol. 327, p. 1631, 2010.

[8] [Online]. Available: http://www.techbriefs.com/component/content/article/17446.

3.3 Fabrication of Demonstration Articles

3.3.1 Demo Overview

The DMLS powder bed method was selected to build the metallurgical and the mechanical test specimens and the demonstration articles. A schematic of the general method for fabrication is depicted in Figure 41a. The powder bed technique has excellent feature resolution and makes complex geometries with ease. This method is the method of choice for alloy development. In the powder bed Laser Direct Manufacturing method, a stationary bed of powdered metal is used as the base for the layered build. The heat source such as a laser spot rapidly ‘draws’ the image of the layer section in the powder bed (Figure 41b), fusing the material into a solid structure. The bed is indexed a small distance, and a doctor blade scrapes a new layer of powder over the surface. The build continues with another melting and fusing powder into shaped structure.

Structures built with powder bed method are typically Hot Isostatic Pressed (HIP) to reduce probability of void presence.

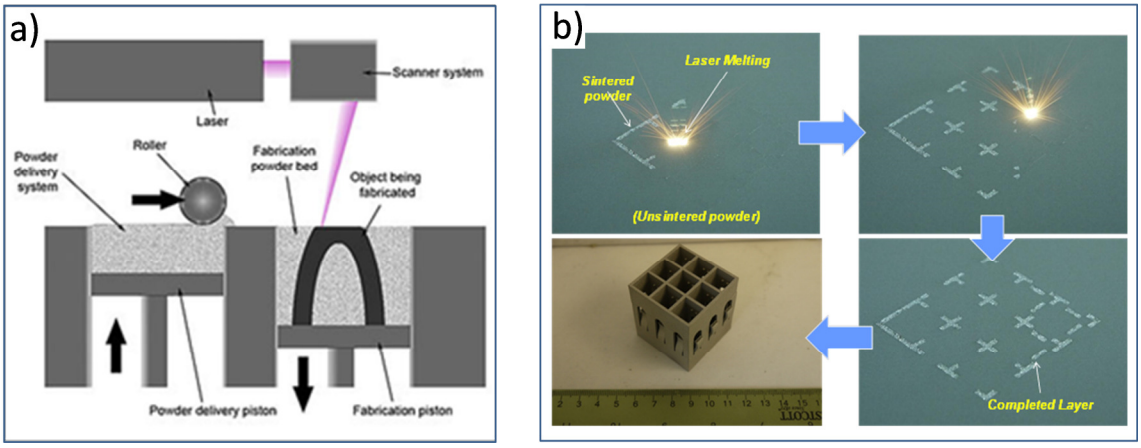

Figure 41. (a) Schematic of the powder bed method; (b) build of a 3x3 spacer grid using powder bed method.

Fabrication of samples began with process trials runs using the Electro Optical Systems (EOS) Direct Metal Laser Sintering (DMLS) system to determine process parameters for each type of material selected. The suite of metal powders used was 316L stainless steel, Inconel 600, Inconel 718, Incoloy 800 and Oxide Dispersed Strengthened (ODS) steel. The critical, variable process parameters were the scan rate and the laser power. The material property used to determine if the parameters were optimized was density (Table 12). Subsequently, the microstructure examination confirmed the parameter selection.

Table 12. Table showing process conditions and parameters varied in process trials.

	Specimen size	Scan speed	Laser power			
Inconel 600	1cmX2cmX1cm	1100mm/s	195W		Standard EOS	
Inconle 718	1cmX2cmX1cm	1200mm/s	195W		Standard EOS	
	1cmX2cmX1cm	1000mm/s	195W	180W	165W	150W
	1cmX2cmX1cm	900mm/s	195W	180W	165W	150W
	1cmX2cmX1cm	800mm/s	195W	180W	165W	150W
	1cmX2cmX1cm	1200mm/s	195W	180W	165W	150W
	1cmX2cmX1cm	1400mm/s	195W	180W	165W	150W

The entry criteria for the manufacturing demonstration of a relevant nuclear reactor component using LDM held two primary imperatives: 1) the component selected for the manufacturing demonstration had to reside within the reactor vessel (and thus be subject to irradiation over its lifetime); and, 2) a standard alloy that is currently used in the construction of reactor internals would be used in the LDM build. Components external to the reactor such as valve assemblies were assessed in the trade space of LDM cost and schedule benefit but were excluded from consideration for this particular demonstration due to the first imperative stemming from guidance provided by the DOE customer team at the original program kickoff.

Available documentation of various nuclear reactor designs was reviewed and discussions with Electric Power Research Institute (EPRI) subject matter experts were held prior to selecting a fuel rod spacer grid for the manufacturing demonstration article. The geometric complexity of spacer grids along with the multi-step machining, joining, and assembly operations required to fabricate them made them ideal candidates for this demonstration. Spacer grid geometric details are typically proprietary to the prime contractors responsible for reactor designs. In the absence of a timely proprietary information sharing agreement with any prime contractor, the LM team decided to generate our own design for a grid with elements, features, and dimensions representative of those found on real reactor hardware. A 3-D solid model isometric representation of the notional spacer grid design is shown Figure 42. The grid was designed at full scale to be a 15x15 cell matrix with flexure elements in each cell. The outer grid dimensions are 7.6in x 7.6in x 1.5in and each cell is approximately 0.5in x 0.5in x 1.5in. Rapid prototyped models of a scaled down 10 x 10 grid, shown in Figure 43, were fabricated to verify the design and desired design features.

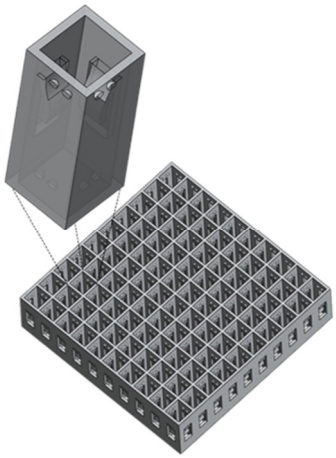

Figure 42. 3-D Solid Model Isometric CAD Drawing Used for Article Build

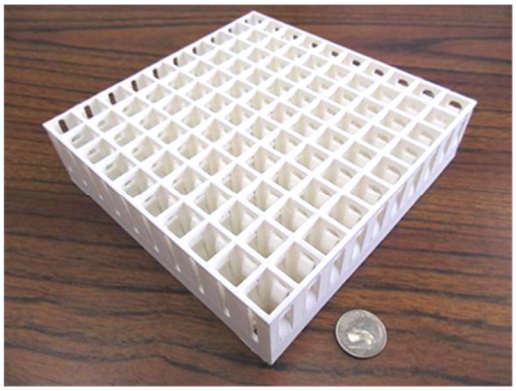

Figure 43. Rapid prototype model of spacer grid designed for manufacturing demonstration

Demonstration articles have been manufactured in three different configurations – 3x3 spacer grid baseline wall thickness and thin wall variations built out of 316LSS, Inconel 600, Inconel 718 and Incalloy 800; an Inconel 600 10x10 grid array with baseline wall thickness and an

Inconel 600 15x15 grid array with reduced wall thickness. Images of the 3x3 316LSS and the 10x10 Inconel 600 grids are shown in Figure 44.

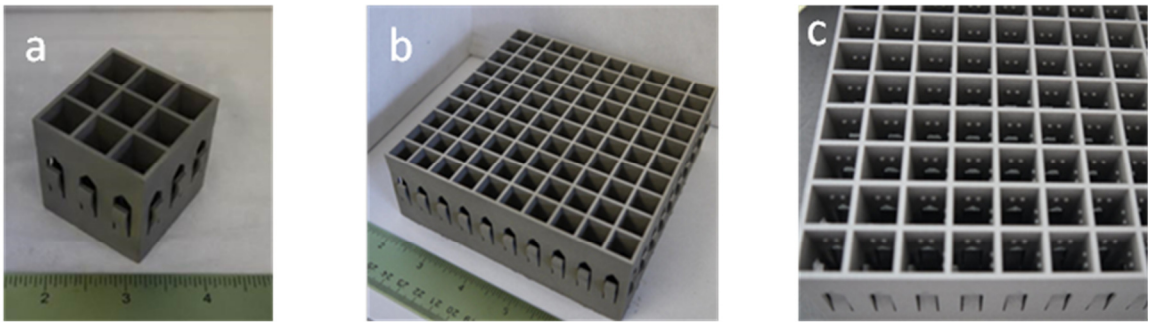

Figure 44. Demonstration articles: (a) 3x3 Inconel grid, (b) 10x10 Inconel grids, (c) 10x10 Inconel spacer grid features.

The spacer grid arrays utilized the optimized process parameters from each trial and the two main types of materials used: 316L SS and the Inconel alloys. Also, a wall thickness study was conducted using the Inconel materials. The wall thickness study was suggested after finding that the actual spacer grid walls are thinner than the 0.063 inch thickness used for the majority of the demonstration articles, fabricated. The 3x3 and 10x10 grid arrays were built with 0.063 inch walls. The wall thickness study focused on two thinner wall dimensions of 0.047 inches and 0.032 inches. Two builds were conducted. A first attempt to build the 3x3 grid with the thinner walls using the same standard re-coater as the baseline was not successful; the thinner walled samples were bent by the standard re-coater (Figure 45a). The second build attempt using a carbon fiber re-coater was successful with both thinner wall thicknesses (Figure 45b).

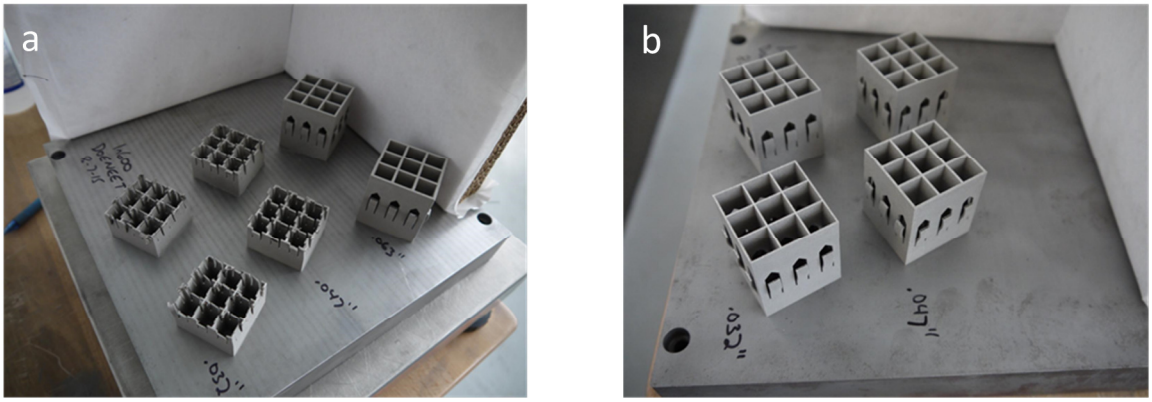

Figure 45. Inconel 600, 3x3 spacer grids: (a) First attempt at thinner walls with standard re-coater showing baseline 0.062" sample and two thinner wall samples at 0.047" and 0.032"; (b) Successful second attempt at thinner wall thicknesses using carbon fiber re-coater application method.

A final spacer grid demonstration piece fabricated in Inconel 600 to demonstrate a nominally standard spacer grid size at 15x15 grid structure. For this build, the narrower 0.032" wall thickness design with the carbon fiber re-coater was utilized. The 15x15 spacer grid assembly is shown in Figure 46.

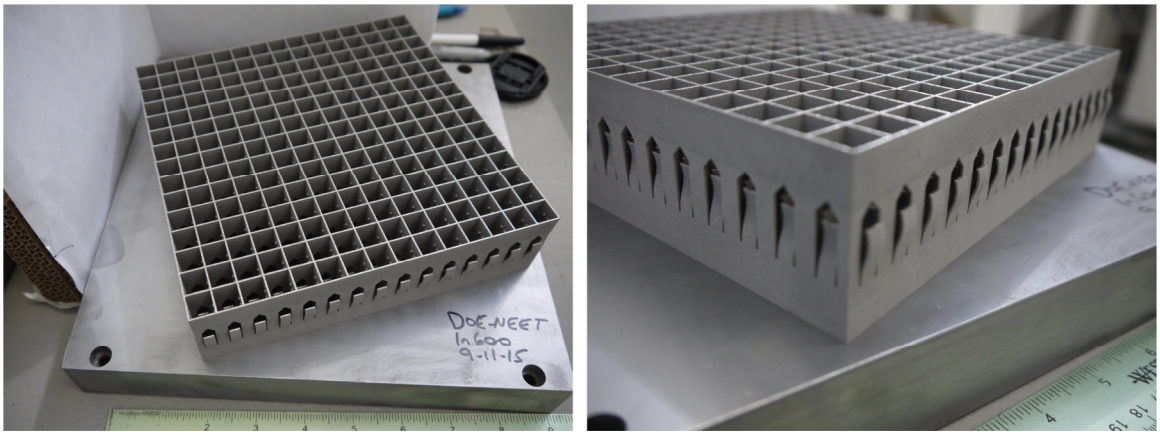

Figure 46. Final demonstration piece using Inconel 600 fabricated in a full 15x15 grid design with the thinner 0.032" wall thickness.

3.4 Manufacturing Case Study

Nuclear power plant components have specialized requirements for performance, durability and longevity. Even seemingly simple components such as plumbing, fittings, valve housings, brackets and vessels must survive aggressive environments with radiation exposure, high temperatures, and high pressures for up to 40 or more years. When these types of requirements are placed on more specialized components with complicated designs such as heat exchangers and turbines, the result is high base manufacturing costs.

Advanced stainless steels and other alloys have been used to meet many power plant component requirements, however higher temperature use, better radiation tolerance, cost and manufacturing lead times are still critical issues. To address the cost and lead time issues in particular, traditional labor-intensive machine shop operations such as machine from billet, machine from forging, or casting may potentially be replaced with Additive Manufacturing (AM) where a part is fabricated directly from a CAD solid model using one of several potential methods.

The following report is an examination of the potential benefits and challenges of AM as it applies generally to the nuclear industry and specifically to a case study of a simple nuclear reactor fuel spacer grid component.

3.4.1 AM Potential Benefits and Challenges for the Nuclear Industry

There are a number of potential areas where AM may provide fabrication cost or technical advantages for nuclear components. Below are just a handful of these:

- Fabricating parts with complex designs that require significant labor, machining, and/or material loss using traditional manufacturing methods.
- Fabricating parts that are not manufacturable using any other known methods.
- Enabling accelerated prototype part design and development.
- Supporting small quantity part builds or quick turns on obsolete parts to reduce outages.
- Fabricating parts from unique materials including difficult to machine materials (ceramics, super alloys, etc.) and Oxide Dispersion Strengthened (ODS) alloys.

- Tailoring microstructure and/or imparting directional dependent properties by modification of AM process parameters.

There are also many challenges associated with implementing AM. It is important to realistically evaluate the benefits of AM compared to traditional methods on a case-by-case basis. Some of the potential challenges a listed below:

- Needed part quantities and part design complexity are key considerations for determining the actual cost to fabricate a part. A determination must be made to see if AM is really cost competitive or if an added cost is worth some other benefit AM can provide.
- Specific part requirements (material properties, dimensional accuracy, etc.) may limit AM method options.
- An AM part may require post processing to meet some specific requirements. For example, finish machining of surfaces requiring high dimensional accuracy.
- It might not be appropriate to utilize AM to fabricate an existing part design.
- New part designs need to take into account the AM fabrication approach for maximum benefit.
- AM is not a 'high volume' production technology at the present time.
- AM cost models tend to be immature due to lack of data and costs are usually based on AM tool build time rates, material use, or qualitative design evaluation.
- Low volume and varied part fabrication makes it difficult to capture all actual costs for a given part.

3.4.2 Example Case Study

3.4.2.1 Cost Model

A simple case study of a representative nuclear reactor component, a generic-design fuel rod spacer grid, was conducted as part of this project. The likely cost elements to manufacture the component using both traditional methods and AM were identified and compared. The example component was then fabricated using a powder bed fusion AM method at the Quad City Manufacturing Lab (QCML) and an estimate of the actual cost was developed based on data collected from the fabrication operation.

A reactor fuel rod assembly end spacer grid was selected as an example component for the case study because it was deemed manufacturable using an existing AM method and is a good candidate for realizing a cost advantage over traditional manufacturing methods. This part has the general characteristics shown below:

- Made from an Inconel alloy
- Has integral springs in each grid element to minimize fuel rod vibration and grid-rod fretting wear induced by coolant flow
- Has defined contact points (lines or dimples) to center the fuel rods in each grid element

Spacer grids have vendor proprietary designs with complicated features, and cost information is not readily available to non-nuclear industry entities. However, discussions with a former Global Nuclear Fuels executive have provided valuable insight into how the grids are currently manufactured.

Basically, traditional spacer grid manufacture consists of hand assembly of pre stamped/machined sections followed by laser welding the sections together. Using this information it was possible to define the likely cost elements associated with the current traditional grid manufacturing approach, and compare them with the cost elements for an AM approach. These are described in the following:

- Part Design and Analysis (Labor)
  - Traditional Manufacture: Grid design, FE modeling for analysis, assembly fixture design, programming the laser welding robot.
  - AM : Grid design, FE modeling for analysis, preparing a part file for AM tool (scale for CTE shrink, add temporary support structures, etc.)
- Raw Materials (Materials)
  - Traditional Manufacture: Inconel bar/plate stock
  - AM : Inconel alloy powder
- Pre Machining (Labor)
  - Traditional Manufacture: Initial machining of subcomponents prior to welding into grid assembly
  - AM : N/A
- Set-Up Hardware and Tooling (Labor)
  - Traditional Manufacture: Set-up or assembly of sub pieces into grid using fixtures
  - AM : Prepare AM tool (set-up platen, load powder, purge, etc.)
- Hardware Run (Capital, Facilities, Labor), usually reduced to a single rate
  - Traditional Manufacture: Laser welding system cost, power usage, purge gas usage, other consumables cost, maintenance/service contract, etc.
  - AM : AM system cost, power usage, purge gas usage, other consumables cost, maintenance/service contract, etc.
- Post Processing (Capital, Facilities, Labor)
  - Traditional Manufacture: Post weld heat treat or stress relief
  - AM : HIP and/or heat treat
- Post Machining (Labor)
  - Traditional Manufacture: N/A or minimal
  - AM : Post machine to remove from platen and clean-up critical locations as needed.
- Quality Check (Labor)
  - Traditional Manufacture: Post fabrication qualification of part (dimensional accuracy check)
  - AM : Post fabrication qualification of part (dimensional accuracy check)
- Scrap (overhead)
  - Traditional Manufacture: Scrap loss
  - AM : Scrap loss

Table 13 summarizes these same major cost elements and identifies a simple cost evaluation formula where known.

Table 13. Summary of Major Cost Elements by Fabrication Method

	Cost Element	Category	Traditional Manufacture	Cost Estimate	Additive Manufacture	Cost Estimate	Comments
1	Design and Analysis	Labor	Grid design, FE modeling for analysis, assembly fixture design, programming/teaching laser welding robot.	(# hrs) x ($__/hr labor rate)	Grid design, FE modeling for analysis, preparing part file for AM tool (scale for CTE shrink, add supports).	(# hrs) x ($__/hr labor rate)	Design is optimized for each fabrication method
2	Raw Materials	Materials	Inconel bar/plate stock	unknown	Inconel alloy powder	(part vol)x(density)x($__/lb metal powder)	
3	Pre Machining	Labor	Initial machining of subcomponents prior to welding into grid assembly	(# hrs) x ($__/hr labor rate)	N/A	N/A	No pre machining for AM part
4	Set-Up	Labor	Set-up or assembly of sub pieces into grid using fixtures	(# hrs) x ($__/hr labor rate)	Prepare AM tool (set-up platen, load powder, purge, etc.)	(# hrs) x ($__/hr labor rate)	Traditional method is skilled labor intensive
5	Hardware Run	Capital, Facilities, Labor	Laser welding system cost, power usage, purge gas usage, other consumables cost, maint/service contract, etc.	(# hrs run time) x ($__/hr)	AM system cost, power usage, purge gas usage, other consumables cost, maint/service contract, etc.	(# hrs run time) x ($__/hr rate)	Data available for AM from QCML
6	Post Processing	Capital, Facilities, Labor	Post weld heat treat or stress relaxation	(# hrs) x ($__/hr rate)	HIP and/or heat treat	(# hrs) x ($__/hr rate)	
7	Post Machining	Labor	N/A or minimal	N/A	Post machine to remove from platen and clean-up critical locations as needed.	(# hrs) x ($__/hr labor rate)	Probably not required for traditional part
8	Quality Check	Labor	Post fabrication qualification of part (dimensional accuracy check)	(# hrs) x ($__/hr labor rate)	Post fabrication qualification of part (dimensional accuracy check)	(# hrs) x ($__/hr labor rate)	Assume same for both
9	Scrap Loss	Materials	Scrap loss	unknown	Scrap loss	unknown	Assume same for both

3.4.2.2 Sample Part

A simple representative 10x10 end spacer grid design was developed that incorporates integral springs and fuel rod positioning dimples. The overall dimensions are 5.19in x 5.19in x 1.75in. A full design analysis including FEM was not performed in this case.

QCML prepared the AM part build file using the provided 3D CAD model and fabricated the part from Inconel-600 powder using an EOSINT M270 powder bed fusion tool. Figure 47 shows a screenshot of the 3D CAD model (in SolidWorks) and the finished AM grid part.

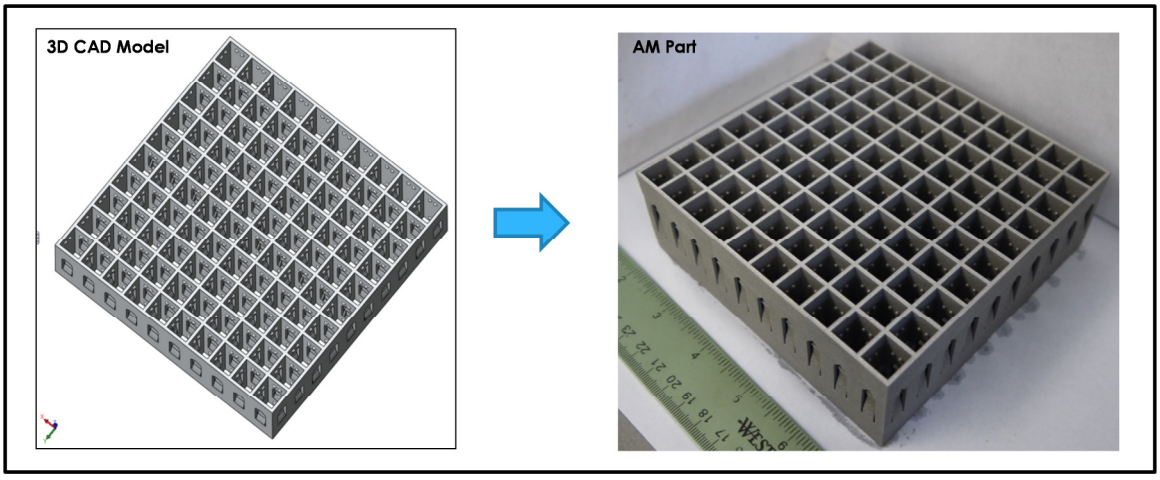

Figure 47 - Simple 10x10 spacer grid design CAD model and finished AM part produced from the model.

Once the AM grid was fabricated it was possible to perform high level cost estimation using the available data. This is summarized below and in Table 14.

- Very minimal time was required for CAD file manipulation, adding supports, scaling, etc. so the Design and Analysis cost was not included. Normally this runs $100/hr.
- The Raw Materials cost for the Inconel-600 powder used in the build was calculated to be $81.75 based on the part volume and a bulk powder cost of $ 25/lb.
- The 10x10 Grid build took 52 hrs. to complete in the QCML EOSINT AM tool and with a run charge rate of $105/hr. gives a Hardware Run cost of $5460.00
- HIP was not performed in this case, but the estimated cost of this Post Processing is $750 and was included in the overall estimate since it would be done in a typical part fab.
- Post Machining (removal from platen and support removal) took approximately 2.5hrs, but the cost is normally rolled into the Hardware Run rate.
- Scrap Loss cost was not evaluated in this case.

Table 14. Cost Element Analysis for AM 10x10 Grid

10 x 10 Grid

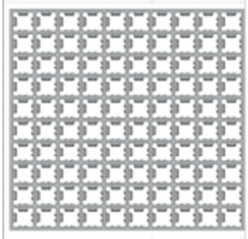

Capacity (rods)	100
Volume (cm3)	176.8
Inconel Density (g/cm3)	8.4
Grid Mass (g)	1485.12
Grid Weight (lbs)	3.27

	Cost Element	Category	Operation	Cost	Comments
1	Design and Analysis	Labor	Grid design, FE modeling for analysis, preparing part file for AM tool (scale for CTE shrink, add supports).	minimal	Modified a pre-existing design variant
2	Raw Materials	Materials	Inconel alloy powder	$81.75	Estimate ~ $25/lb
3	Pre Machining	Labor	n/a	n/a	none required
4	Hardware Set-up	Labor	Prepare AM tool (set-up platen, load powder, purge, etc.)	Included	Design Provided, cost covered in build rate
5	Hardware Run	Capital, Facilities, Labor	AM system cost, power usage, purge gas usage, other consumables cost, maint/service contract, etc.	$5,460.00	52 hr build
6	Post Processing	Capital, Facilities, Labor	HIP and/or heat treat	$750.00	Assumed cost, but not actually performed
7	Post Machining	Labor	Post machine to remove from platen and clean-up critical locations as needed.	Included	cost covered in build rate
8	Quality Check	Labor	Post fabrication qualification of part (dimensional accuracy check)	Included	cost covered in build rate
9	Scrap Loss	Materials	Scrap loss	-	not evaluated
			Total Part Cost:	$6,291.75	

3.4.2.3 Manufacturing Case Study Summary

Basic fabrication cost elements were identified to facilitate general comparisons between a Traditionally Manufactured part and an Additively Manufactured part. These were based on discussions with knowledgeable personnel and common sense assumptions. The cost to fabricate a simple fuel rod spacer grid using AM was estimated to be $6291.75 from available data from an actual build of the part at QCML.

Unfortunately, direct cost comparisons between traditional manufacturing methods and AM are challenging because of the limited data openly available for traditionally manufactured parts and the lack of precise cost models for additive manufacturing.

3.4.2.4 Path Forward for Manufacturing Modeling

There are several actions that could further the implementation of AM for use in the nuclear power industry. These actions include:

- Develop a more comprehensive understanding of the present and future nuclear industry part needs in general.
- Identify cases where additive manufacturing might be appropriate or recommended for nuclear related part fabrication. This would involve developing a parts or subcomponent

list, and defining part complexity, costs to manufacture, known current problems and/or failure mechanisms, quantities needed, etc.
- Educate part designers to identify cases where AM might make sense and create designs that leverage AM advantages
- Investigate the potential for using AM in the case of as-needed obsolete parts replacement
- Develop more detailed business cases and collect additional data to be able to create mature cost models for AM.

3.5 Outreach & Technology Transfer Activities

During the program, special consideration was paid to identifying ways to utilize resources available to the team to network, augment the program capabilities, and improve the overall conceptual development of LDM to meet the objectives of addressing the benefits of LDM to meet the nuclear power community needs. Discussions early in the program focused mainly on identifying industry needs and helping to vector the efforts of the program. As the program progressed and new networking opportunities presented themselves, new collaborators were engaged to assist in identifying new possibilities for leveraging the effort of the program to solve challenges in the nuclear community and to improve the overall understanding of the additive manufacturing as it pertains to the nuclear industry. Below is a list of key connections that were made during the program:

- Ames Laboratory – Dr. Iver Anderson at Ames Lab was engaged as an option for the formulation of ODS powders for LDM. The gas atomization reaction synthesis process his team has developed at Ames was under consideration as an ODS metal powder source.
- Electric Power Research Institute (EPRI) – Industry perspectives were important in the early phase of the program to identify relevant reactor internal components to fabricate for demonstration purposes. Input from EPRI was critical in assisting that decision. Later discussions were held that pertained to future phases of development, beyond the scope of this program that would be relevant to the nuclear community.
- Flurry Powders, LLC. – Flurry was a collaborator on the development of ODS powder formulations using their spray drying technique to agglomerate oxide and steel powders.
- General Electric (GE) Global Research – LM has been asked by Dr. Xiao Lou at GE to transfer Inconel 800 samples and unused Inconel 800 powder from the LM NEET effort to GE under the recently awarded GE NEET program in support of additive manufacturing development for nuclear components. LM has requested permission and at this time is awaiting approval. GE plans to use the same collaborate as LM, Quad City Manufacturing Laboratories (QCML), to fabricate Inconel 800 samples for test and evaluation.
- Idaho National Laboratory (INL) – INL was integral in the early program discussions regarding material selection for the LDM trade study on materials for development. In addition, members of the LM team attended the Advanced Test Reactor (ATR) users' meeting to gain background on options for radiation test and characterization at the INL ATR complex. LM reached out to colleagues in the Light Water Reactor Sustainability Program to discuss high level approaches to implementing LDM and the general benefits of additive manufacturing.
- Massachusetts Institute of Technology (MIT) – LM met with Professor Baglietto of the Nuclear Engineering Department to discuss collaborative opportunities for marrying the

LDM approach for prototype development with the modeling and simulation work on fluid flow through reactor cores as a way to optimize reactor internal component design. There is promise in this area for reducing the cost of design and prototype fabrication of new and more complex reactor internal components.

- NIST Center for Neutron Research – The NIST neutron beam user facility has the ability to map internal stresses using one of the beam lines. LM discussed with NIST the possibility of collaboration and may still do so under the effort with Texas A&M.
- Oak Ridge National Laboratory (ORNL) – At one point, LM had discussions with Dr. Jeremy Busby of ORNL about the possibility of setting up an additive manufacturing workshop between LM and ORNL. Scheduling challenges ultimately resulted in this workshop being postponed to a yet to be determined time. Discussions were also held to discuss possible future phases of additive development and its relevance to both the nuclear and aerospace communities.
- Texas A&M University – Lockheed Martin is working with Professor Sean McDeavitt and his graduate students to irradiate and perform post-irradiation evaluations of samples fabricated under the LM NEET program. Permission was requested from the Department of Energy and granted for LM to transfer samples to Texas A&M for insertion into the TRIGA test reactor at Texas A&M and for ion beam irradiation testing.
- Westinghouse Electric Company – Early stage discussions were held to assist in identifying components and materials of interest for fabrication. Additional discussions were held in the late stages of the program to discuss potential path forwards for the additive manufacturing in the nuclear industry.

All of the relationships described above, at one time or another throughout the program, proved valuable in meeting the objectives of developing and assessing the benefits of additive manufacturing or the nuclear community. In addition, LM is working with QCML and Texas A&M to publish two papers on (1) the development and fabrication of samples and demonstration pieces, and (2) the irradiation, test and characterization of irradiated samples.

No inventions or patent applications were filed as a result of this effort.

4.0 Path Forward and Future Work

The LDM approach was investigated under the NEET program to explore the development of additive manufacturing methods that have matured within the aerospace and other industries and can be applied to the needs of the nuclear community. As with any program, there are always areas that, in hindsight, could have benefitted from additional focus. In addition, there are areas that were outside the scope of this program, but are now closer to being realized thanks to both the progress made within this effort and the progress made within the community at large. The suggestions hear are areas that LM views as essential to maturing additive manufacturing for use within the nuclear community.

- Materials and alloy development
    - Further characterization at the nanoscale
    - Powder formulation
    - ODS process development
- Design base maturation
    - Improved designs based on additive approach
    - Newly enabled designs thanks to additive manufacturing

- Manufacturing maturation
    - Improved process development
    - In-situ process monitoring
    - Predictive model development
    - Feedback control
- Radiation test and characterization
    - Correlation of radiation performance to nanoscale material characteristics
    - Characterization of nominal alloys
    - Investigations into nano-tailored alloys and designs
- Continued study of the business case development and maturation
- Nuclear component additive manufacturing standards development and process/parts qualification

For the nuclear industry, LDM promises faster build schedules, reduced costs and rapid prototyping of complex components. Novel and challenging parts for improved performance can be tested quickly and with high fidelity. Digital design optimization can be combined with simulation to dramatically improve new reactor designs, fluid flow performance and overall reactor safety. Additive manufacturing is completing overhauling the way all industries approach development and manufacturing. The Department of Energy and the nuclear industry is right in being active in repeating those benefits for the nuclear power community. Through this and new efforts currently funded through NEET, the community is better positioned to reap these benefits.